Politecnico di Torino

Master's Degree Program in Civil and Environmental Engineering
A.y. 2025/2026
Degree Examination Session March 2026

Preliminary study for the development of a hydraulic model of the Cavour Canal

Supervisors:

Prof.ssa Stefania Tamea
Prof.ssa Ilaria Butera
Doc. Matteo Carollo

Candidate:

Gabriele Francione

Preliminary study for the development of a hydraulic model of the Cavour Canal

Gabriele Francione

Abstract

The thesis presents a preliminary study about a major hydraulic infrastructure that is the Cavour Canal, a water distribution work that supports the irrigation of a major area in the north of Piemonte. First, historical documentation was considered to frame the infrastructure development and to define the channel layout, the design slopes and the geometric characteristics of the channel cross section. This information is then complemented with ground elevation information and aerial overviews. Water inflows and outflows of the canal and the most significant hydraulic nodes associated to them —such as branch canals and irrigation ditches— were examined in order to get a preliminary understanding of the variations in discharge along the entire course of the Cavour Canal. The HEC-RAS model was selected for hydraulic simulations, and a set-up has been created with the collected information and estimation of missing parameters. Some analyses were performed on the results including simulated flows along the channel. Quantitative information provided by irrigation consortia were helpful to get realistic simulations from the one-dimensional analysis of a six-year study period.

Contents

List of Tables

List of Figures

1 Introduction

The Cavour Canal is one of Piedmont's major hydraulic infrastructures and its importance lies in its connection to a larger irrigation water distribution system. To study its hydraulic behavior, it is necessary to develop a model that approximates its actual behavior and must take into account the structure of the irrigation distribution system, study the canal conditions due to the operation of the floodgates, which can cause flooding and water shortages and study the seasonal trends of actual flow rates. The proposed model takes into account historical design data, the geometric characteristics of the canal and available quantitative hydrometric data.

1.1 The History of the Cavour canal

The history of the Cavour canal, the subject of this thesis, begins around 1840, when Francesco Rossi from Vercelli was the first to conceive its construction. The project was commissioned by the Prime Minister of the Kingdom of Sardinia, Count Camillo Benso di Cavour (after whom the canal is named) and entrusted to the engineer Carlo Noè. Noè's design placed the canal's origin in Chivasso, from where it would continue through the central Vercelli area, the Novara area, and Lomellina, with the aim of irrigating a vast portion of the plain before finally flowing into the Ticino River. The Italian Parliament approved the project in 1862, shortly after the proclamation of the Kingdom of Italy, and its construction cost approximately forty-five million lire.

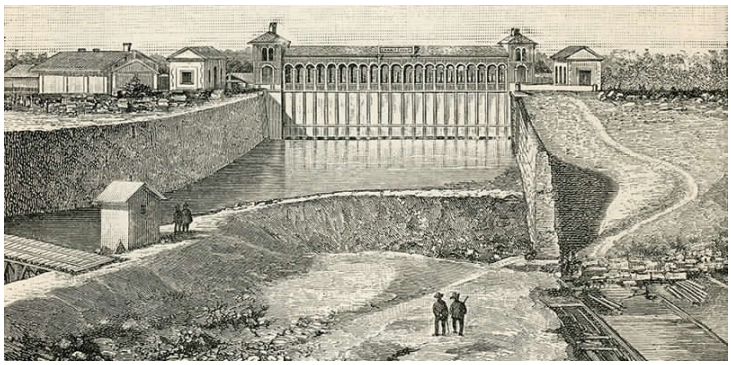

Figure 1: Cavour canal

Until 1977, management of the canal was entrusted to the Amministrazione generale dei canali demaniali d'irrigazione, after which the Coutenza Canali Cavour was established. This body, still active today, also manages other canals in the area and it is composed by two geographical consortium, Ovest and Est Sesia. [1]

The Cavour canal stretches for 83 km, and at its intake in Chivasso from the Po River, it was designed to have a maximum flow rate of $110\,m^3/s$, which can decreases to $85\,m^3/s$ near Novara.

[1] https://coutenzacanalicavour.it/

1.2 Definitions

- **Subsidiary canals**:

  A canal is subsidiary if it supplies the main canal to which it is connected with all or part of its flow rate.

- **Branch canals**:

  A branch canal is a branch of the main canal that transports water to more specific areas of a hydraulic network, typically in irrigation or water distribution systems.

- **Concession flow rate**:

  The concession flow rate is the maximum authorized flow rate that can be withdrawn or conveyed in the canal according to the administrative concession.

- **Derived flow rate**:

  It is the flow that is subtracted from the current of the main canal to feed the branch canals. It depends on variables such as the water level of the Cavour canal and the geometry of the floodgate.

- **Inlet flow rate**:

  It is the quantity of water that is introduced into a canal thanks to the water supply of the subsidiary canals connected to it.

- **Lateral outlet floodgates**:

  Structures located near the bank of the main canal and in correspondence with a branch canal. Their opening varies the derived flow rate value.

- **Inlet hydraulic nodes**:

  Structures located at the end of the subsidiary canals and in correspondence with the main canal which they feed with the intake of the inlet flow rate.

1.3 Geometric data of the Cavour canal

The intake structure of the canal is located on the Po River, in the city of Chivasso. From the intake point, the canal intersects numerous watercourses along its route, which are crossed by means of highly complex hydraulic works. The Dora Baltea is spanned by an aqueduct bridge, at which point the subsidiary Farini canal also joins; the Ivrea canal is crossed in elevation, while the Elvo Stream is passed beneath through a siphon culvert.

Continuing into the Vercellese area, the canal passes beneath the Cervo Stream and reaching kilometer 55 it meets the Sesia River, also crossed by means of a large siphon culvert. Entering the Novara area, the canal intersects the Busca and Biraga irrigation ditches and, further downstream, the Agogna Stream. Beyond Novara, two main branch canals diverge: the Quintino Sella and the Vigevano after which the main course ends in the Ticino River.

The riverbed, with an initial bottom width of 40 meters (a), gradually narrows to 20 meters (b) with a slope of 0.25‰, then to 12.50 meters (c) after the intersection with the

Busca ditch, and finally to 7.50 (d) meters after crossing the Terdoppio river. The banks, lined with concrete, have a slope of 1:1.5 and a variable height from 2.70 to 4 meters.

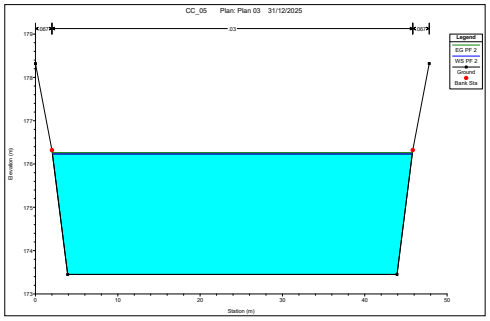

(a) Riverbed width 40 m

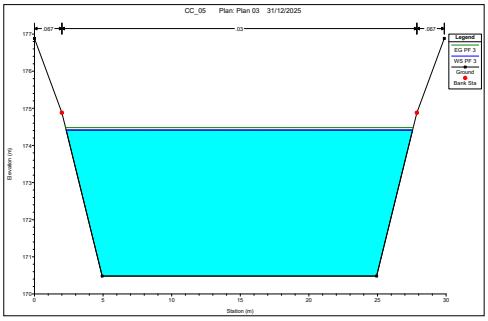

(b) Riverbed width 20 m

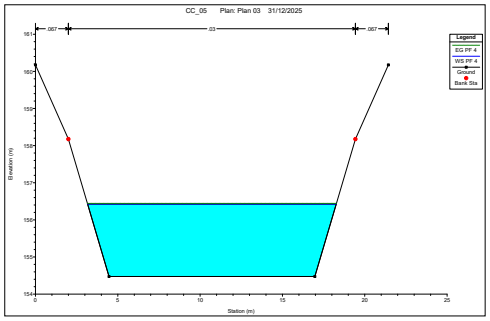

(c) Riverbed width 12.5 m

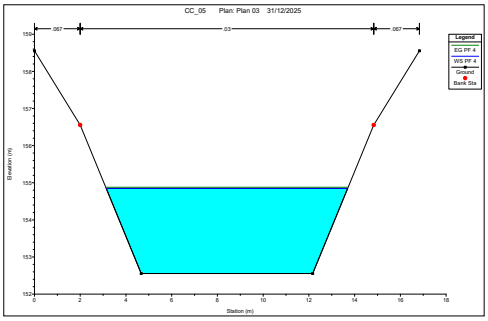

(d) Riverbed width 7.5 m

2 Topographic data of the Cavour Canal

The Cavour canal crosses the territories of twenty-three municipalities in Piedmont, and its course had to take into account the region's topography in order to ensure a constant hydraulic load along the entire length of the canal.

It is useful in this regard to define the concept of the elevation of a point and, in particular, to distinguish between orthometric height, ellipsoidal height, and geoid undulation. [2]

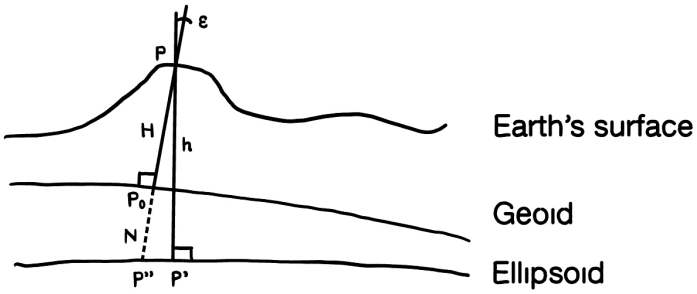

Figure 3: Elevation of a point

The geoid can be defined as the equipotential surface that passes through mean sea level, while the reference ellipsoid is a mathematically defined surface obtained by rotating an ellipse around one of its principal axes in order to approximate the geoid.

The orthometric height of a point P indicates its distance from the geoid measured along the plumb line orthogonal to the geoid itself, while the ellipsoidal height of P indicates its distance from the ellipsoid measured along the normal. It follows that the geoid undulation is given by the difference between the orthometric height and the ellipsoidal height.

The elevation difference can instead be defined as the difference in orthometric height between two points; in this way, the elevation difference is positive or negative depending on whether the height of the second point is greater or smaller than that of the first.

$$\Delta_{AB} = z_B - z_A$$

Let us now recall the methods of measuring elevation differences that may have been used in the years immediately preceding the construction of the canal. We distinguish between direct and indirect leveling: the former are measurements independent of distance and include geometric, hydrostatic, and barometric leveling; on the other hand, assuming the measurement of the distance between the two points, we have indirect leveling methods such as stadia leveling and trigonometric leveling.

Since all the instruments useful for leveling were already in use by 1840, the designers could choose whether to use a level and leveling rods (geometric leveling), simulate a system of communicating vessels (hydrostatic leveling), take measurements with a barometer

[2] G. Comoglio. Topografia e cartografia. Celid, 2006.

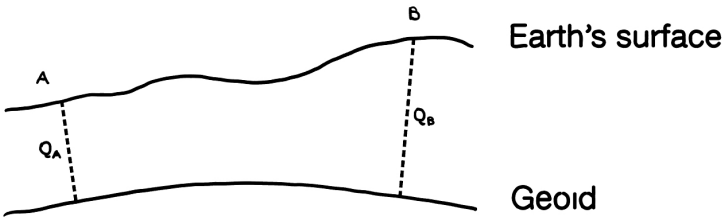

Figure 4: Elevation difference

(barometric leveling), or use theodolites and distance meters (stadia and trigonometric leveling).

Once the methods of measuring the elevation difference between two points are known, and the distance between them is also known, it is possible to obtain the hydraulic gradient i, which is given by the ratio between the elevation difference (rise or fall) and the horizontal distance covered, and is usually expressed as a percentage.

$$i = -\frac{\partial h}{\partial s} \Longleftrightarrow \begin{cases} \Omega = cost \\ Q = cost \end{cases} \Longrightarrow U = cost$$

Moreover, according to Bernoulli's theorem [3], the piezometric head h is given by the sum of the orthometric height z and the piezometric height p/γ; the latter term is also called the pressure head and, in the case of uniform flow in open-canal currents, it depends on atmospheric pressure. It follows that the only variable parameter in choosing the river course is the geodetic height; thus, if the elevations of the Piedmontese municipalities are known, it is possible to identify the ideal route by connecting municipalities with progressively decreasing heights above mean sea level.

$$h = z + \frac{p}{\gamma}$$

[3]D. Citrini and G. Noseda. Idraulica. CEA, 1987.

Analyzing the current route, it is observed that the canal passes through the territories of three Piedmontese provinces, namely the Metropolitan City of Turin, the Province of Vercelli, and the Province of Novara.

The municipalities crossed by the canal are: Chivasso, Verolengo, Saluggia, Lamporo, Livorno Ferraris, Bianzè, Tronzano Vercellese, Crova, San Germano Vercellese, Santhià, Casanova Elvo, Formigliana, Balocco, Villarboit, Albano Vercellese, Greggio, Recetto, Biandrate, Vicolungo, San Pietro Mosezzo, Novara, Cameri, and Galliate.

Table 1: Elevations of the areas crossed by the Cavour canal

Province	City	Orthometric Height m	Elevation Difference m	Geographic Position
Torino	Chivasso	175.00	-	$45°11'01''N\ 7°53'43''E$
Torino	Verolengo	179.42	4.42	$45°11'43''N\ 7°57'53''E$
Vercelli	Saluggia	172.70	-6.72	$45°12'49''N\ 8°02'07''E$
Vercelli	Lamporo	173.31	0.61	$45°14'26''N\ 8°05'01''E$
Vercelli	Livorno Ferraris	172.67	-0.64	$45°16'03''N\ 8°07'32''E$
Vercelli	Bianzè	170.13	-2.54	$45°17'23''N\ 8°09'23''E$
Vercelli	Crova	168.19	-1.94	$45°19'55''N\ 8°12'29''E$
Vercelli	San Germano Vercellese	168.14	-0.05	$45°21'17''N\ 8°13'42''E$
Vercelli	Casanova Elvo	166.57	-1.57	$45°23'40''N\ 8°14'40''E$
Vercelli	Formigliana	165.45	-1.12	$45°25'50''N\ 8°17'06''E$
Vercelli	Balocco	161.90	-3.55	$45°26'41''N\ 8°17'45''E$
Vercelli	Villarboit	161.47	-0.43	$45°26'34''N\ 8°20'31''E$
Vercelli	Albano Vercellese	164.22	2.75	$45°26'55''N\ 8°21'40''E$
Vercelli	Greggio	164.81	0.59	$45°27'19''N\ 8°22'44''E$
Novara	Recetto	160.29	-4.52	$45°27'17''N\ 8°26'11''E$
Novara	Biandrate	161.59	1.30	$45°27'30''N\ 8°27'42''E$
Novara	Vicolungo	158.92	-2.67	$45°27'42''N\ 8°29'11''E$
Novara	San Pietro Mosezzo	160.47	1.55	$45°28'00''N\ 8°31'20''E$
Novara	Vignale	159.96	-0.51	$45°28'45''N\ 8°36'32''E$
Novara	Cameri	160.89	0.93	$45°29'16''N\ 8°39'47''E$
Novara	Galliate	155.49	-5.40	$45°29'12''N\ 8°42'39''E$

2.1 Design data of the Cavour canal

More accurate measurements were taken once the localities were selected. These new values were used for the historical project, and are still available. Among these values there are the orthometric heights taken at 500 meters from the canal axis which are reported in the following table;

Table 2: Design Heights

First Orthometric Height m	Second Orthometric Height m	Elevation Difference m	Reach Lenght m
178.61	178.12	0.49	1000
178.12	176.72	1.39	2000
176.72	176.77	-0.05	7473
176.77	171.47	5.30	2300
171.47	165.72	5.75	26647
165.72	165.25	0.47	180
165.25	164.59	0.66	900
164.59	164.30	0.29	1000
164.30	165.22	-0.93	1500
165.22	164.85	0.37	1610
164.85	164.09	0.76	2910
164.09	163.38	0.71	7620
163.38	163.38	0.00	270
163.38	163.12	0.26	1090
163.12	160.71	2.41	1500
160.71	160.49	0.22	1000
160.49	158.79	1.70	3570
158.79	159.28	-0.49	8030
159.28	159.27	0.01	1400
159.27	158.20	1.07	1910
158.20	156.36	1.84	4090
156.36	153.19	3.16	4230
153.19	128.48	24.72	0

The reach lenghts reported on Tab. 2 are referred to the height measurements. From their sum the stationing distances of canal Cavour are ordered from downstream to upstream. In the following table these lenghts are coupled with the respective canal-bed width allowing for the evaluation of each canal cross section.

Table 3: Stationing and canal bed widths

Reach lenght m	Stationing distance m	Canal bed width m
1000	82230	40
2000	81230	35.56
7473	79230	26.67
2300	71757	20
26647	69457	20
180	42810	20
900	42630	20
1000	41730	20
1500	40730	20
1610	39230	20
2910	37620	20
7620	34710	20
270	27090	20
1090	26820	20
1500	25730	20
1000	24230	20
3570	23230	20
8030	19660	20
1400	11630	12.5
1910	10230	12.5
4090	8320	12.5
4230	4230	7.5
0	0	7.5

3 Free Surface Currents

Since the Cavour channel currents are free-surface currents, the equations governing these flows are introduced below.

3.1 De Saint-Venant

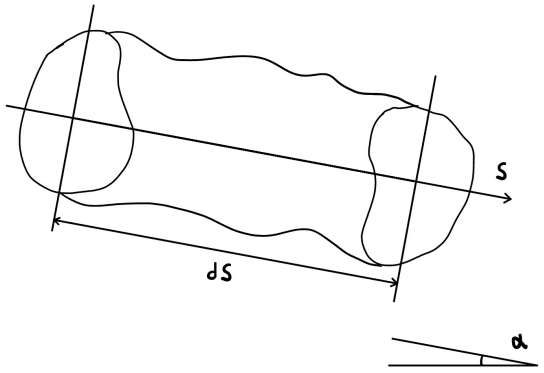

Figure 5: De Saint-Venant Model

Acceleration along s:

$$A_s = \frac{\partial U}{\partial t} + U\frac{\partial U}{\partial s}$$

Newton's law:

- ρ = fluid's density
- ds = variation in space
- Ω = surface area
- U = velocity

$$\sum_{n=1}^{\infty} F_{s,i} = dm\ A_s = \rho\,\Omega\,ds\ \left(\frac{\partial U}{\partial t} + U\frac{\partial U}{\partial s}\right)$$

Mass forces:

- γ = specific weight of the fluid
- $\Omega\,ds$ = volume
- $\frac{\partial z}{\partial s} = sin\ \alpha$

$$P = -\gamma\,\Omega\,ds\frac{\partial z}{\partial s}$$

Surface forces comprises:

1. hydrostatic thrust variation along two sections of the model:

$$\Pi_1 - \Pi_2 = p\Omega - \left(p\Omega + \frac{\partial p\Omega}{\partial s}ds\right) = \left(-p\frac{\partial \Omega}{\partial s} - \Omega\frac{\partial p}{\partial s}\right)ds$$

2. longitudinal component of the tangential tension:

   - τ_0 = tangential tension
   - $\mathcal{P}$ = wet perimeter

$$T_x = -\tau_0\,\mathcal{P}\,ds$$

3. perpendicular component of the tangential tension:

$$T_y = p\frac{\partial \Omega}{\partial s}ds \begin{cases} > 0 \;\; if \;\; \Omega \;\; expands \;\; along \;\; ds \\ < 0 \;\; if \;\; \Omega \;\; decreases \;\; along \;\; ds \end{cases}$$

The model equation becomes:

$$P + \Pi_1 - \Pi_2 + T_x + T_y = F_{s,i}$$

$$-\gamma\,\Omega\,ds\frac{\partial z}{\partial s} - p\frac{\partial \Omega}{\partial s}ds - \Omega\frac{\partial p}{\partial s}ds - \tau_0\,\mathcal{P}\,ds + p\frac{\partial \Omega}{\partial s}ds =$$

$$= \rho\,ds\,\Omega\,\left(\frac{\partial U}{\partial t} + U\frac{\partial U}{\partial s}\right)$$

Dividing all terms by $(-\gamma\,\Omega\,ds)$ the equation simplifies:

$$\Longrightarrow \frac{\partial z}{\partial s} + \frac{1}{\gamma}\frac{\partial p}{\partial s} + \frac{\tau_0\mathcal{P}}{\gamma\,\Omega} + \frac{1}{g}\left(\frac{\partial U}{\partial t} + U\frac{\partial U}{\partial s}\right) = 0$$

Two assumptions are made:

1. the fluid is incompressible $\Longrightarrow \frac{\partial\, h}{\partial\, s}$
2. energy grade line is parallel to free-water surface $\tau_0 = \gamma\frac{\Omega}{\mathcal{P}}i \Longrightarrow \frac{\tau_0\,\mathcal{P}}{\gamma\,\Omega} = i = J$

Replacing:

$$\frac{\partial\, h}{\partial\, s} = \frac{\partial z}{\partial s} + \frac{1}{\gamma}\frac{\partial\, p}{\partial\, s}\; and\; J = \frac{\tau_0\mathcal{P}}{\gamma\,\Omega}$$

$$\Longrightarrow \frac{\partial\, h}{\partial\, s} + J + \frac{1}{g}\frac{\partial\, U}{\partial\, t} + \frac{U}{g}\frac{\partial\, U}{\partial\, s} = 0$$

$$\Longrightarrow \frac{\partial\, h}{\partial\, s} + \frac{1}{g}\frac{\partial\, U}{\partial\, t} + \frac{\partial\, U^2}{\partial s\, 2g} = -J$$

By deriving the piezometric head along space:

$$h = Y + z_f \Longrightarrow \frac{\partial h}{\partial s} = \frac{\partial Y}{\partial s} + \frac{\partial z_f}{\partial s} \Longrightarrow \frac{\partial z_f}{\partial s} = -i_f$$

$$\Longrightarrow \frac{\partial Y}{\partial s} + \frac{\partial z_f}{\partial s} + \frac{\partial}{\partial s}\frac{U^2}{2g} + \frac{1}{g}\frac{\partial U}{\partial t} = -J$$

$$\Longrightarrow \frac{\partial Y}{\partial S} + \frac{\partial}{\partial s}\frac{U^2}{2g} + \frac{1}{g}\frac{\partial U}{\partial t} = i_f - J$$

The continuity equation for an incompressible fluid ($\rho = 0$) becomes:

$$\frac{\partial\, \rho Q}{\partial\, s} + \frac{\partial\, \rho \Omega}{\partial\, t} = 0 \Longrightarrow \frac{\partial\, Q}{\partial\, s} + \frac{\partial\, \Omega}{\partial\, t} = 0$$

Combining the two equations results in the De Saint-Venant Model:

$$\begin{cases} \frac{\partial Y}{\partial S} + \frac{\partial}{\partial s}\frac{U^2}{2g} + \frac{1}{g}\frac{\partial U}{\partial t} = i_f - J \\ \frac{\partial\, Q}{\partial\, s} + \frac{\partial\, \Omega}{\partial\, t} = 0 \end{cases}$$

3.2 Uniform flow

The Cavour canal flow can be approximated with uniform flow if the assumptions that allows for the approximation are satisfied; in particular the uniform flow requires:

$$\frac{\partial}{\partial t} = \frac{\partial}{\partial s} = 0 \; and \; \begin{cases} \frac{\partial Y}{\partial S} + \frac{\partial}{\partial s}\frac{U^2}{2g} + \frac{1}{g}\frac{\partial U}{\partial t} = i_f - J \\ \frac{\partial Q}{\partial s} + \frac{\partial \Omega}{\partial t} = 0 \end{cases} \implies i_f = J$$

Rigorously, this would mean that there are no variations along the sections of the canal and that there are no variations in flow rate over time. Also the slope of the piezometric head has to be exactly equal to the slope of the canal bottom and this is insured by having only one specific canal velocity U that satisfy this condition. When for example there is a variation of the canal geometry, mathematically this case would belong to permanent flow $\left(\frac{\partial}{\partial t} = 0\right)$ but for the project of an artificial canal this case can be neglected having the uniform flow more stringent conditions.

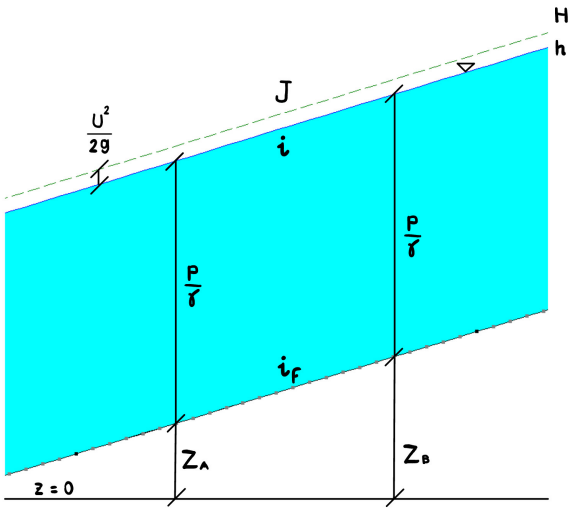

Figure 6: Uniform Flow Profile Example

The Chezy equation for Uniform Flow velocity is:

$$U = \chi\sqrt{\mathcal{R}\, i_f}$$

where:

- $\mathcal{R} = \frac{\Omega}{\mathcal{P}}$ = hydraulic radius
- χ = Chezy roughness coefficient, which can be selected from:
  - $k_s\, \mathcal{R}^{\frac{1}{6}}$ Gauckler-Strickler;
  - $\frac{\sqrt{8g}}{\sqrt{\lambda}}$ Colebrook;
  - $\frac{1}{n}\, \mathcal{R}^{\frac{1}{6}}$ Manning;

Knowing that:

$$\Longrightarrow \begin{cases} Q = U\,\Omega \\ \Omega = f(Y) \end{cases}$$

The flow rate formula can be derived from the Chezy uniform velocity equation:

$$Q = \Omega\,\chi\sqrt{\mathcal{R}\,i_f}$$

And so the flow curve (Y, Q) is governed by the integral in space:

$$Q = \iint U(x,y)\,dx\,dy$$

4 Subsidiary and branch canals

To address flow shortage of the Cavour canal, due to summer droughts at the Po river in Chivasso, several supplementary works were undertaken to stabilize and increase the water supply. In 1868, the subsidiary Farini canal was constructed, drawing from the Dora Baltea and capable of diverting water into the Cavour, thus compensating for the summer low flows of the Po (Fig.7). At the same time, work began on the distribution network: in the same year, the Montebello ditch and the Galliate consortium ditch were opened, providing water to the Novara and Lomellina territories.(Fig.15)

The most significant addition was the construction of the Quintino Sella Branch canal, (Fig. 11) completed in 1871. With its more than twenty-three kilometers in length, it enabled improved irrigation distribution and also the exploitation of water drops for energy purposes. In the years immediately following, the system was extended with sub-branches toward Pavia and Mortara, further expanding the irrigated area.

In this way, thanks to a series of complementary works, the system gradually approached the flow originally stipulated by the 1862 convention, namely 90 cubic meters per second beyond the Sesia. In addition to the direct diversions from the Po at Chivasso and from the Dora Baltea through the Farini, the Cavour canal also received, over time, contributions from the Ticino thanks to the Diramatore Alto Novarese (Fig. 9) and the Regina Elena canals (Fig. 10). This was made possible in 1954 through the regulation of Lake Maggiore at Miorina and the release of water into the canal via the Veveri outlet. In this way, the Cavour's capacity to ensure extensive and continuous irrigation of the Novara and Lomellina territories was definitively consolidated, overcoming the limitations that had marked its early years. [4]

[4]https://www.ovestsesia.it/storia/canale-cavour/

4.1 Farini subsidiary canal

The first hydraulic work supplying the Cavour canal when proceeding downstream from Chivasso is the Farini canal. It connects to the Cavour canal approximately 12 km from Chivasso, near the town of Saluggia. The canal is named after Luigi Carlo Farini, Prime Minister of the Kingdom of Italy. The Farini canal was constructed in 1868 in order to increase the discharge of the Cavour canal, which initially suffered from water shortages during the summer months due to the presence of a single intake from the Po River. Through the Farini canal, the cold water from the Dora Baltea River can be diverted, ensuring adequate flow conditions in the Cavour canal under all hydrological scenarios. The main characteristics of the Farini canal are its relatively short length, approximately 3 km, and its considerable width of about 35 m, which locally reaches dimensions comparable to the riverbed of the Dora Baltea. The initial value of discharge used for the simulations is set at 10 m^3/s and is consistent with the quantitative data of the Ovest Sesia consortium. [5] [6]

Figure 7: Farini - 1:1000

[5] https://www.parcopopiemontese.it/pun-dettaglio.php?id=970
[6] https://www.ovestsesia.it/

4.2 Ivrea subsidiary canal

Similarly to the Farini canal, the Ivrea canal also originates from the Dora Baltea River, but much further upstream, specifically within the historic center of Ivrea. It terminates in Vercelli, where it discharges into the Sesia River. The canal was originally constructed in 1468 by the House of Savoy as a navigable link between Ivrea and Vercelli. Today, it primarily supplies irrigation water to the rice fields of the Vercelli plain. From Masino, the canal follows the Masino moraine and subsequently runs alongside the Dora Baltea for several kilometers, intersecting first the Depretis canal and then reaching the town of Santhià. The Ivrea canal continues until it meets the Cavour canal, where, at approximately 34 km from Chivasso, it contributes part of its discharge through the Naia Hydraulic Node. For the evaluation of its discharge, a conservative value of 10 m^3/s is taken into account to comply with the concession flow rate. [7]

Figure 8: Ivrea Canal - 1:1000

[7] https://it.wikipedia.org/wiki/Naviglio-di-Ivrea

4.3 Alto Novarese subsidiary canal

The Alto Novarese subsidiary canal originates from the Regina Elena canal and has an average discharge of approximately 25 m^3/s. It is about 21 km long and has an average width of roughly 10 m. Following a series of enlargement works carried out by the Est Sesia Irrigation Consortium, the canal became operational in 1981. Along its course, it crosses the Terdoppio and Agogna streams by means of siphon culverts, while it overpasses the Mora–Strona ditch via an aqueduct bridge. The canal terminates by discharging into the Cavour canal at Recetto, approximately 68 km from Chivasso. In recent years, an additional hydraulic structure has been constructed to allow part of the Alto Novarese discharge to supply the Montebello canal. [8]

Figure 9: Alto Novarese subsidiary canal - 1:1000

[8] https://it.wikipedia.org/wiki/Diramatore-Alto-Novarese

4.4 Regina Elena subsidiary canal

The Regina Elena canal flows entirely within the Province of Novara. Its construction began in 1938 and was completed in 1954. The canal is 25 km long and has a discharge of approximately 70 m^3/s at its intake from the Ticino River, which decreases to about 45 m^3/s downstream of the diversion to the Alto Novarese subsidiary canal. The Regina Elena canal discharges into the Cavour canal in order to supply its downstream reach and mitigate water shortages during drought periods. The confluence occurs approximately 74 km from Chivasso, just upstream of the Quintino Sella and Vigevano branch canals. [9]

Figure 10: Regina Elena - 1:500

[9] https://it.wikipedia.org/wiki/Canale-Regina-Elena

4.5 Quintino Sella branch canal

The Quintino Sella branch canal was constructed between 1870 and 1874, following the completion of the Cavour canal. It supplies irrigation water to the provinces of Novara and Pavia and derives its discharge directly from the Cavour canal. The canal has a width of approximately 10 m, a depth exceeding 3 m, and a maximum discharge of up to 38 m^3/s. It branches off from the Cavour canal about 74 km downstream of Chivasso, near Veveri, north of Novara, immediately after the inflow from the Regina Elena canal. Downstream, the Quintino Sella canal divides into two sub-branches: the Pavia sub-branch, flowing toward the city of Pavia, and the Mortara sub-branch, directed toward Mortara. The canal is used for irrigation purposes as well as for hydroelectric power generation and hosts several fish species. [10]

Figure 11: Inlet of the Quintino Sella canal - 1:500

[10] https://it.wikipedia.org/wiki/Canale-Quintino-Sella

4.6 Vigevano branch canal

The Vigevano branch canal was constructed in 1868 and was originally known as the Belletti Ditch. It has an average discharge of approximately 22 m^3/s and a total length of 29 km. The canal branches off from the Cavour canal about 81 km downstream of Chivasso, near the municipality of Galliate in the Province of Novara. Along its course, it supplies the Cerana ditch and overpasses the Moretta ditch before eventually discharging into the Pavia sub-branch canal. [11]

Figure 12: Vigevano Branch canal - 1:1000

[11] https://it.wikipedia.org/wiki/Diramatore-Vigevano

4.7 Busca branch canal

The Busca ditch was originally constructed by the city of Novara in the 14th century and was initially known as the Novarese ditch. In the 17th century, ownership passed to Count Ludovico Busca, from whom the ditch takes its present name. The ditch crosses the provinces of Novara and Pavia and originates from the Sesia River near the municipality of Ghemme. It has a total length of 54 km and an average width of approximately 9 m. The Busca ditch crosses the Cavour canal at around 62 km from Chivasso by means of a siphon culvert, but it also receives a water subsidy from the Cavour canal, reaching a downstream discharge of approximately 34 m^3/s. Further downstream, it intersects the Biraga ditch and continues southward into the Lomellina area. [12]

Figure 13: Busca Ditch - 1:1000

[12]https://it.wikipedia.org/wiki/Roggia-Busca

4.8 Biraga branch canal

The Biraga Ditch, like the Busca, is of ancient origin and was constructed in the 15th century by the city of Vercelli. Part of its route runs parallel to that of the Busca Ditch. It originates from the Sesia River and subsequently crosses first the Alto Novarese subsidiary canal and then the Cavour canal at approximately 60 km from Chivasso. Downstream of the Cavour canal, it receives a discharge subsidy, reaching a flow rate of about 27 m^3/s and an average width of approximately 10 m. The ditch then intersects the Busca Ditch and continues until it splits into two outlets, one discharging into the Sesia River and the other into the Agogna Stream. It supplies three hydroelectric power plants and is used for irrigation by the Est Sesia Consortium. [13]

Figure 14: Biraga Ditch - 1:500

[13] https://it.wikipedia.org/wiki/Roggia-Biraga

4.9 Montebello branch canal

The Montebello canal is an irrigation canal constructed in 1868 and named after a battle of the Second Italian War of Independence. It flows within the Province of Novara and branches off from the Cavour canal at approximately 68 km from Chivasso, near the municipality of Recetto. Since 1980, following the completion of the Alto Novarese subsidiary canal, the Montebello canal has also been supplied by the latter, reaching a discharge of approximately 10 m^3/s. [14]

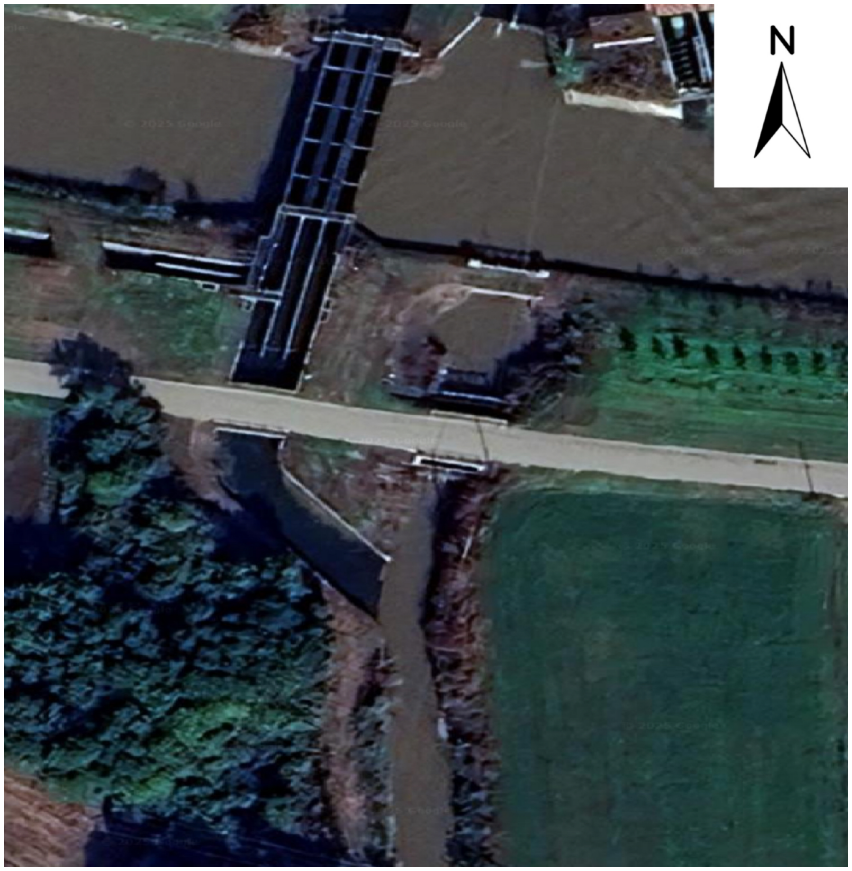

Figure 15: Montebello canal - 1:500

[14] https://it.wikipedia.org/wiki/Cavo-Montebello

4.10 Lucca branch canal

The Lucca canal is an artificial canal branching off from the Cavour canal at approximately 22 km from Chivasso and is managed by the Ovest Sesia Irrigation Consortium. It was constructed in 1922 in the municipality of Livorno Ferraris. The canal is approximately 3 km long and has a discharge ranging between 6 and 8 m^3/s. It terminates in the Saluggia Naviletto, where it supplies the Lucca Hydroelectric Power Plant, operational since 2004 with an installed capacity of 506 kW. [15]

Figure 16: Lucca canal - 1:1000

[15] https://www.ovestsesia.it/centrali/lucca/

5 Analysis of hydrometric measurements

5.1 Lucca canal hydrographs

The hydrograph of the Lucca canal represents the temporal evolution of discharge from 2019 to 2024. This hydrograph has been obtained using interpolation in order to reconstruct missing data and fill temporal gaps.

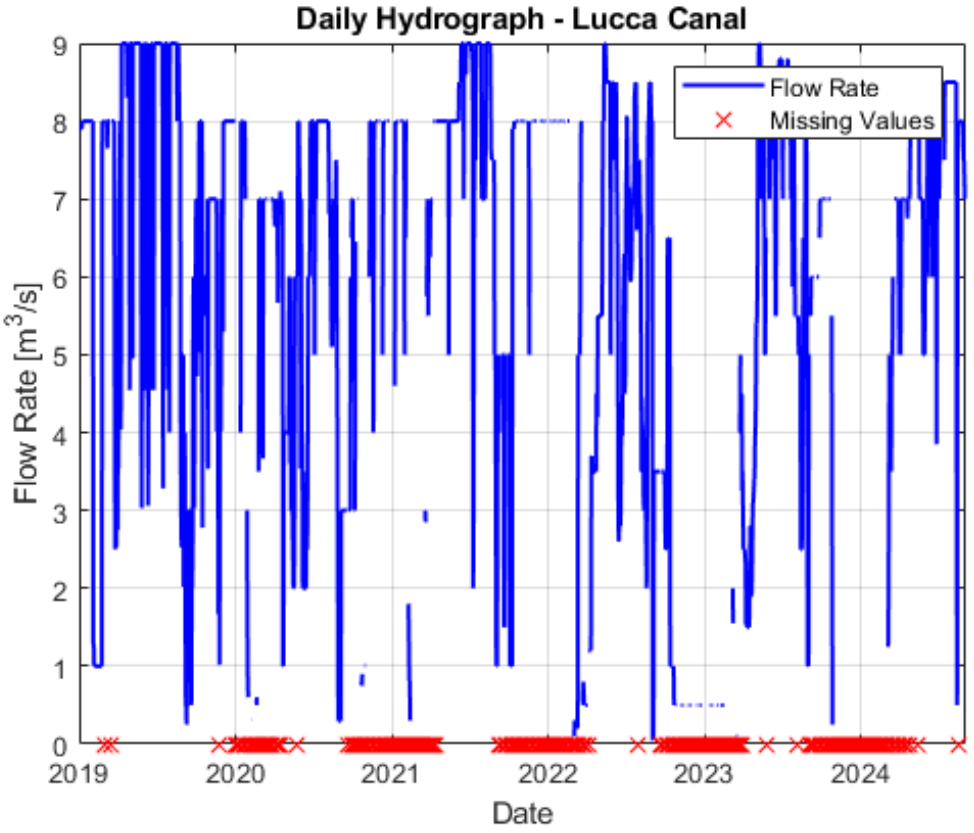

Figure 17: Lucca Hydrograph with missing values

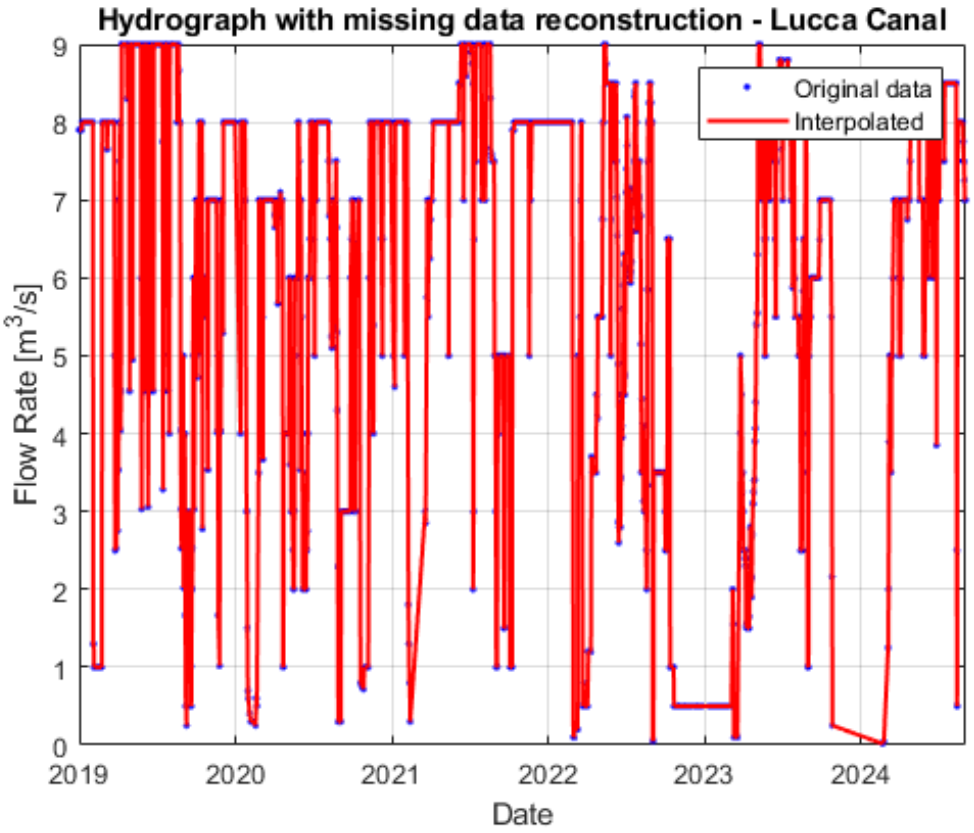

Figure 18: Lucca Hydrograph

5.1.1 Mean Annual Discharge

The mean annual discharge of the Lucca canal has been calculated starting from the average values of each year, and then the mean of all years is calculated.

$$Q_{mean,year} = \frac{1}{n} \sum_{i=1}^{n} Q_i$$

$$Q_{MAD} = \frac{1}{N} \sum_{j=1}^{N} Q_{mean,year}$$

Table 4: Mean Annual Discharge Lucca

Year	Mean
2019	6.78
2020	5.33
2021	6.67
2022	4.42
2023	3.80
2024	5.37
TOTAL	5.39

5.1.2 Regime Curve

The regime curve of the Lucca canal shows the average seasonal variation of stream flow. It is obtained by plotting all monthly discharge values together and then computing the mean discharge for each month.

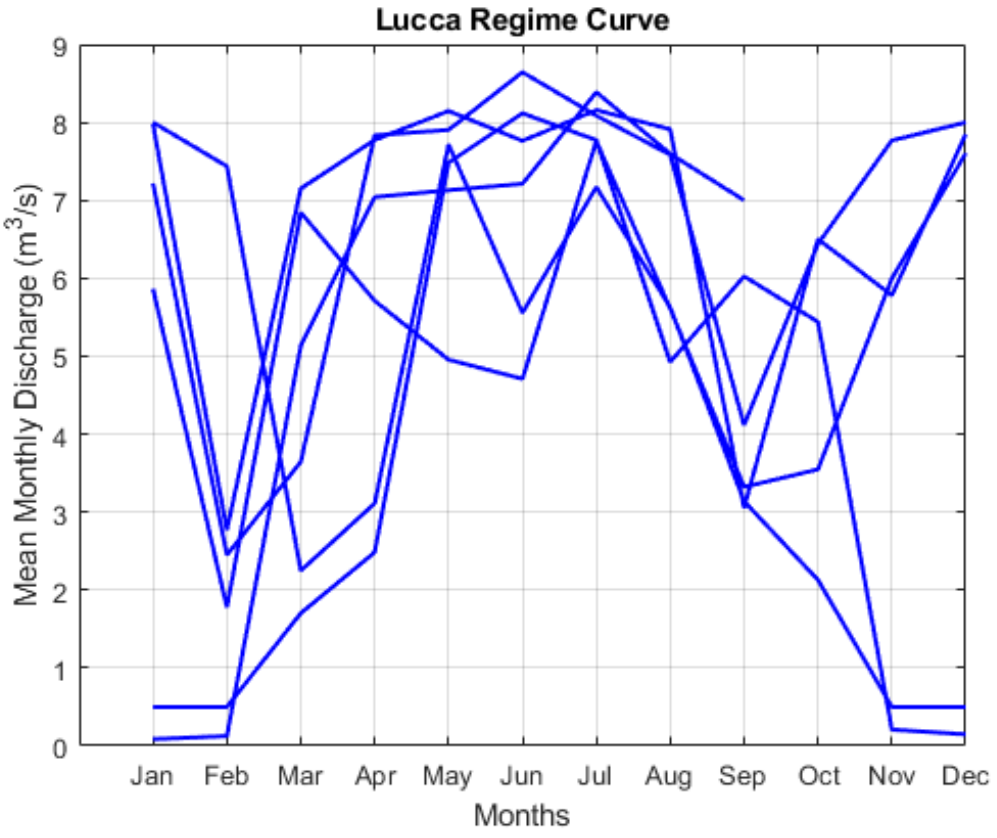

Figure 19: Lucca Regime Curve

5.1.3 Flow Duration Curve

The long term Flow Duration Curve of the Lucca canal combines the discharge values from January 2019 to September 2024 and their exceedance probabilities.

Discharge values were listed in descending order without regard to the sequence of occurrence.

To every value a rank m was assigned in order to calculate the exceedance probability through the Weibull equation $P = \frac{m}{n+1}$;

n = Number of discharge values;

m = Average rank. For equal values of discharge:

$m = \frac{r_i + r_f}{2}$; r_i = Rank of the first value; r_f = Rank of the last value;

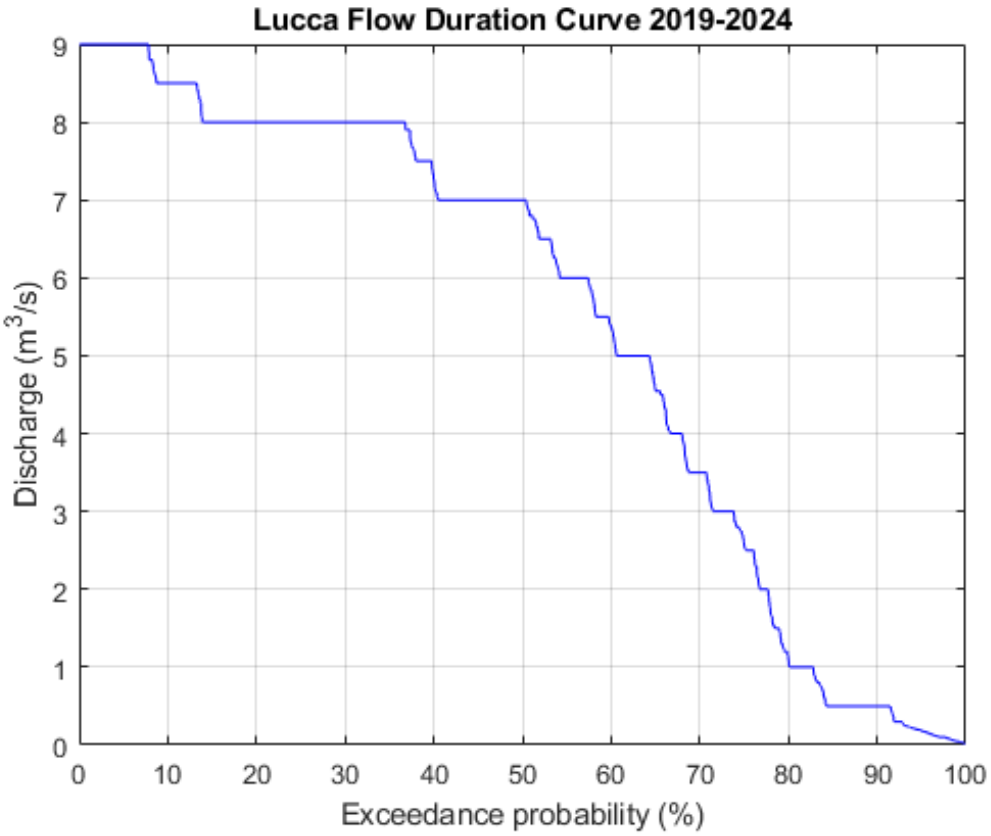

Figure 20: Lucca Flow Duration Curve

5.2 Farini canal hydrographs

The hydrograph of the Farini canal covers the period from 2019 to 2024 and illustrates the changes in discharge over time. Fig. 21. This values have also been interpolated to fill temporal gaps. Fig. 22 The data was given in MOD equivalent to $100\,l/s$ and later converted in m^3/s for comparison with the Cavour's hydrograph.

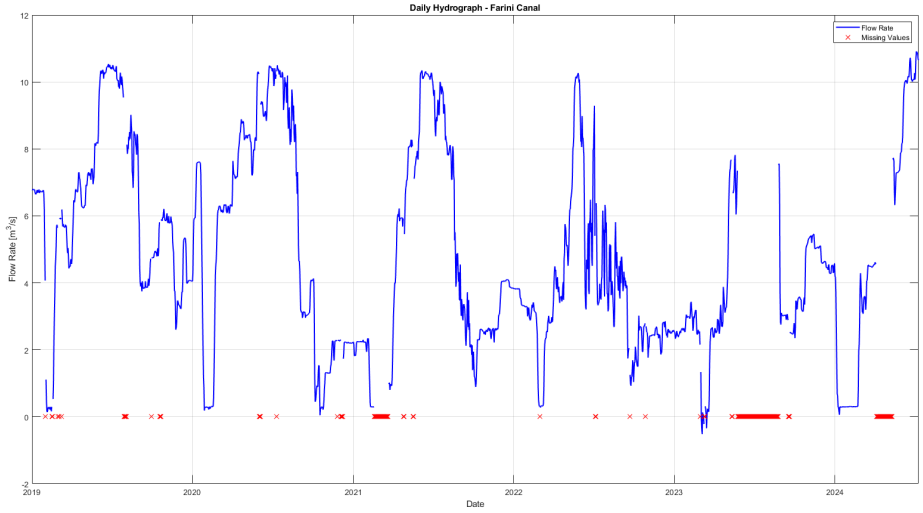

Figure 21: Farini hydrograph with missing values

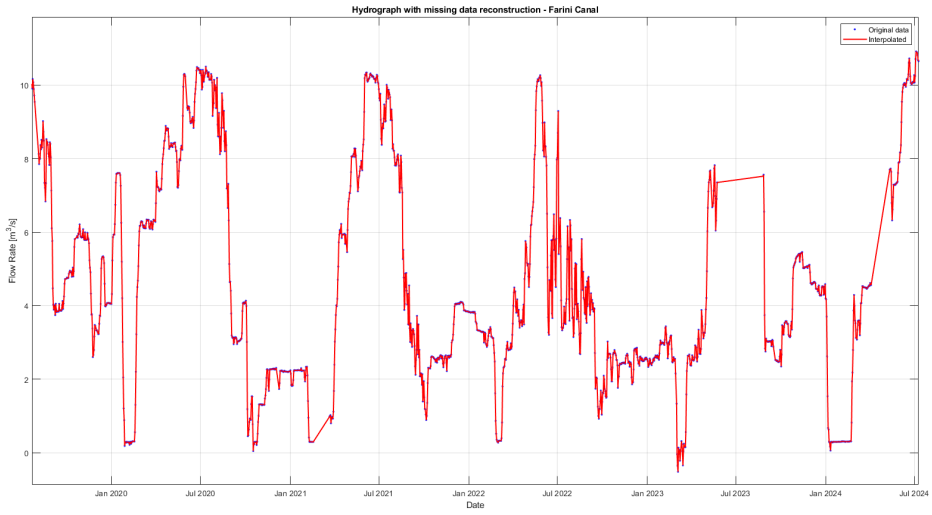

Figure 22: Farini hydrograph

5.2.1 Mean Annual Discharge

The mean annual discharge of the Farini canal has been calculated starting from the average values of each year, and then the mean of all years is calculated.

$$Q_{mean,year} = \frac{1}{n}\sum_{i=1}^{n} Q_i$$

$$Q_{MAD} = \frac{1}{N}\sum_{j=1}^{N} Q_{mean,year}$$

Table 5: Mean Annual Discharge Farini

Year	Mean
2019	6.25
2020	5.53
2021	4.54
2022	3.80
2023	4.53
2024	5.04
TOTAL	4.95

The values calculated in Tab. 5 show that the time period 2022-2023 has the lowest discharge values for the Farini canal; the mean discharge value for the time period 2022-2023 is:

$$Q_{mean} = \frac{Q_m^{2022} + Q_m^{2023}}{n_{years}} = \frac{3.80 + 4.53}{2}\, m^3/s = 4.17\, m^3/s$$

5.2.2 Regime Curve

The regime curve of the Farini canal shows the average seasonal variation of stream flow. It is obtained by plotting all monthly discharge values together and then computing the mean discharge for each month.

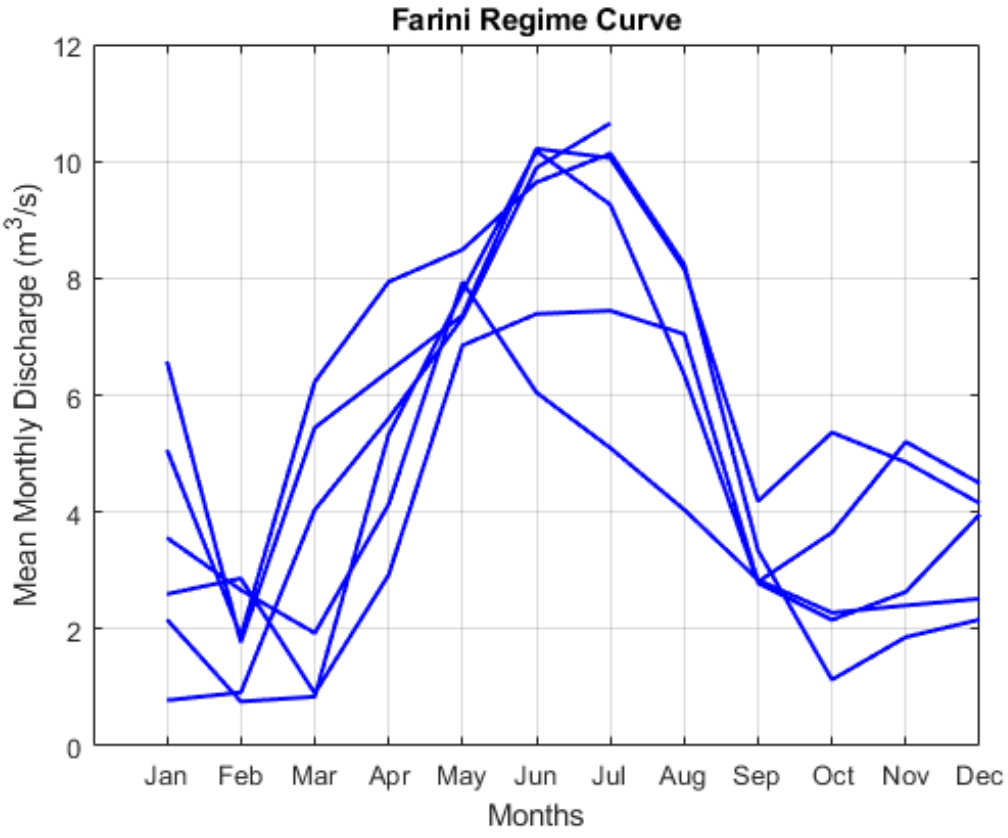

Figure 23: Farini Regime Curve

5.2.3 Flow Duration Curve

The long term Flow Duration Curve of the Farini canal combines the discharge values from January 2019 to September 2024 and their exceedance probabilities.

Discharge values were listed in descending order without regard to the sequence of occurrence.

To every value a rank m was assigned in order to calculate the exceedance probability through the Weibull equation $P = \frac{m}{n+1}$;

n = Number of discharge values;

m = Average rank. For equal values of discharge:

$m = \frac{r_i + r_f}{2}$; r_i = Rank of the first value; r_f = Rank of the last value;

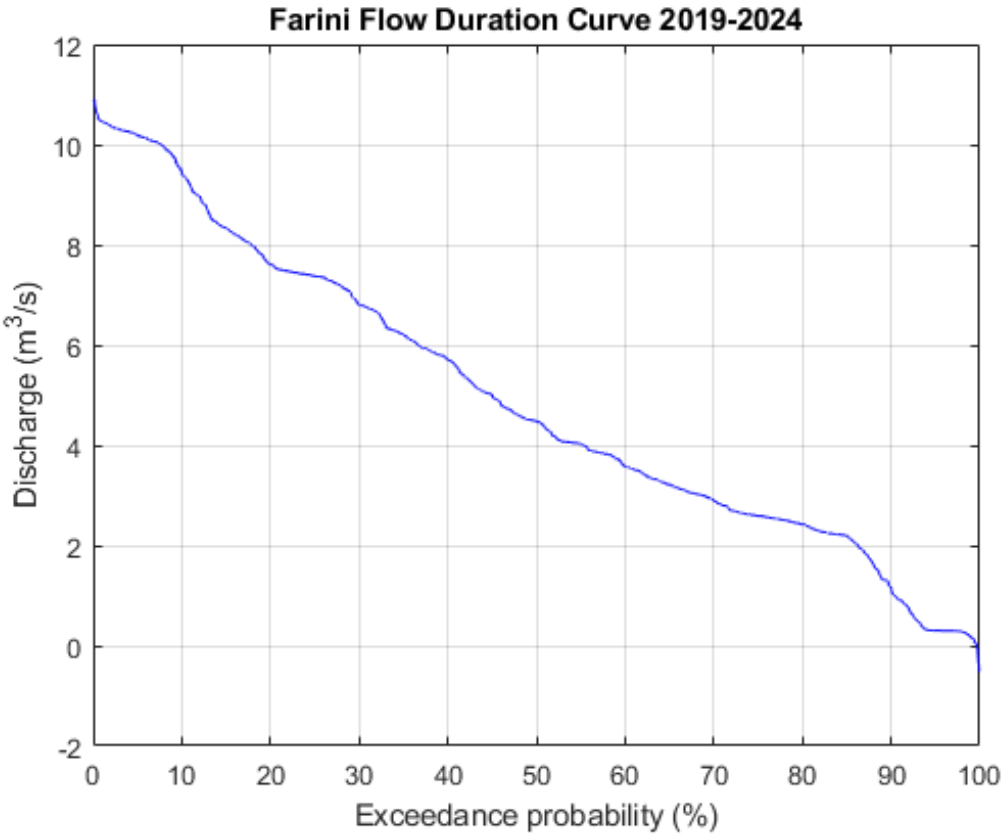

Figure 24: Farini Flow Duration Curve

5.3 Cavour canal hydrographs

Similarly, the Cavour canal's hydrograph shows discharge variations from 2019 to 2024. Fig. 25 The hydrograph was derived from regional temporal data registered in the Cavour canal after the Farini subsidy and was later interpolated like the previous cases. Fig. 26. [16]

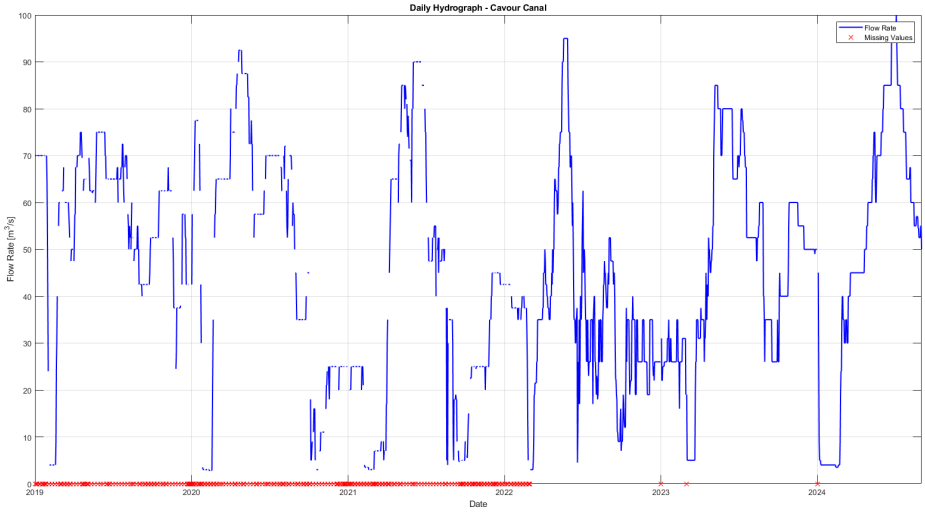

Figure 25: Cavour hydrograph with missing values

The results obtained thanks to the hydrometric measurements allow for the temporal analysis of flow rate values. The frequency of precipitation and the contribution of the inflow and outflow canals influence the results. Fig 26

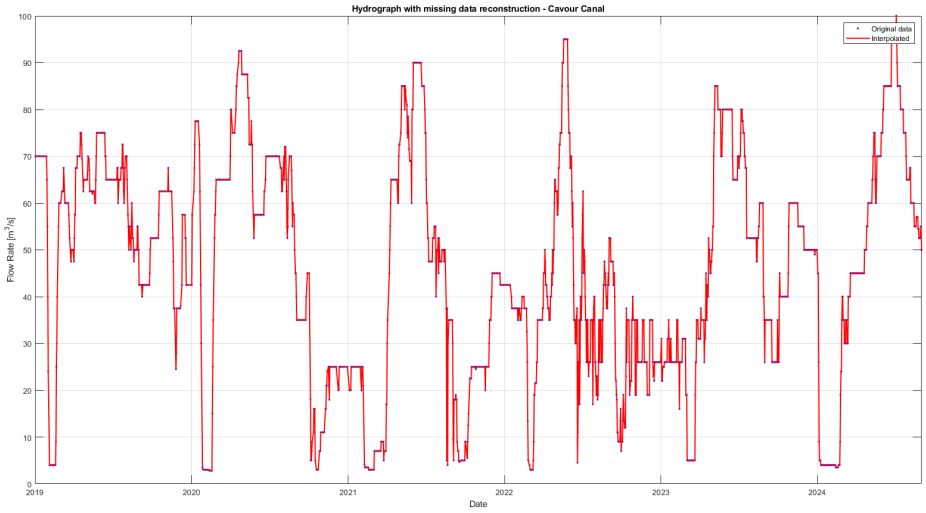

Figure 26: Cavour hydrograph

[16] https://www.arpa.piemonte.it/dati

5.3.1 Mean Annual Discharge

The mean annual discharge of the Cavour Canal has been calculated starting from the average values of each year, and then the mean of all years is calculated.

$$Q_{mean,year} = \frac{1}{n}\sum_{i=1}^{n} Q_i$$

$$Q_{MAD} = \frac{1}{N}\sum_{j=1}^{N} Q_{mean,year}$$

Table 6: Mean Annual Discharge Cavour

Year	Mean
2019	55.79
2020	48.62
2021	37.95
2022	36.65
2023	46.53
2024	50.01
TOTAL	45.93

The values calculated in Tab. 5 show that the time period 2021-2022 has the lowest discharge values for the Cavour canal; the mean discharge value for the time period 2021-2022 is:

$$Q_{mean} = \frac{Q_m^{2021} + Q_m^{2022}}{n_{years}} = \frac{37.95 + 36.65}{2}\ m^3/s = 37.30\ m^3/s$$

5.3.2 Regime Curve

The regime curve of the Cavour canal shows the average seasonal variation of stream flow. It is obtained by plotting all monthly discharge values together and then computing the mean discharge for each month.

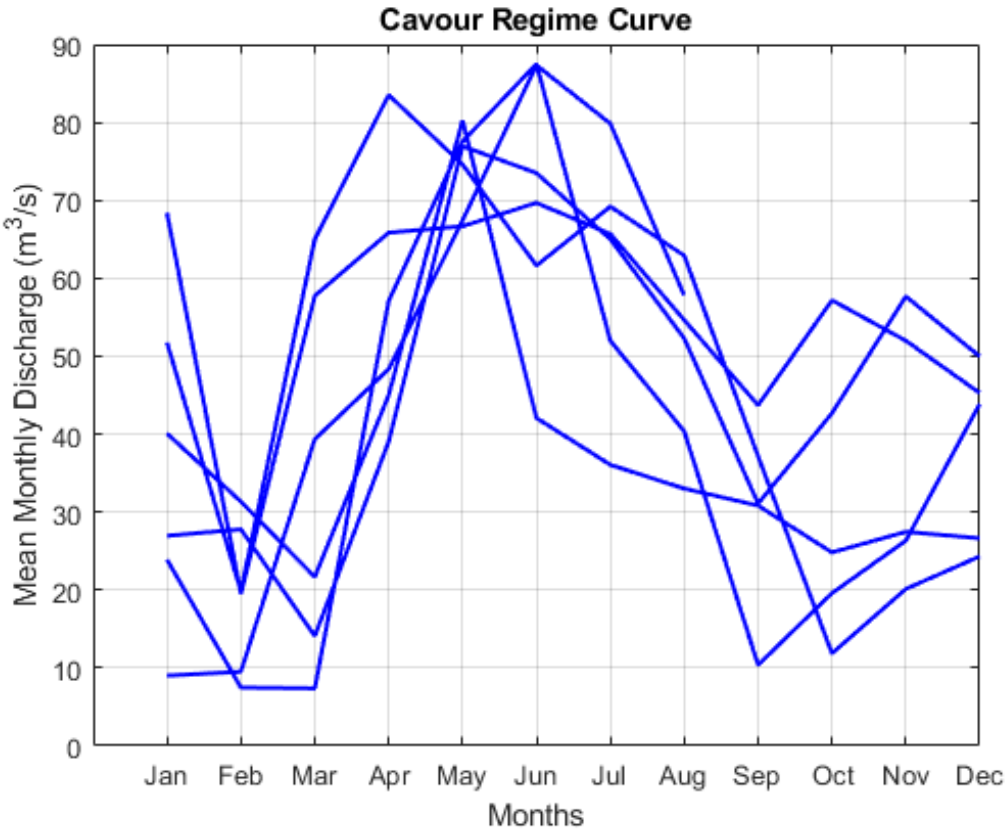

Figure 27: Cavour Regime Curve

5.3.3 Flow Duration Curve

The long term Flow Duration Curve of the Cavour canal combines the discharge values from January 2019 to September 2024 and their exceedance probabilities.

Discharge values were listed in descending order without regard to the sequence of occurrence.

To every value a rank m was assigned in order to calculate the exceedance probability through the Weibull equation $P = \frac{m}{n+1}$;

n = Number of discharge values;

m = Average rank. For equal values of discharge:

$m = \frac{r_i + r_f}{2}$; r_i = Rank of the first value; r_f = Rank of the last value;

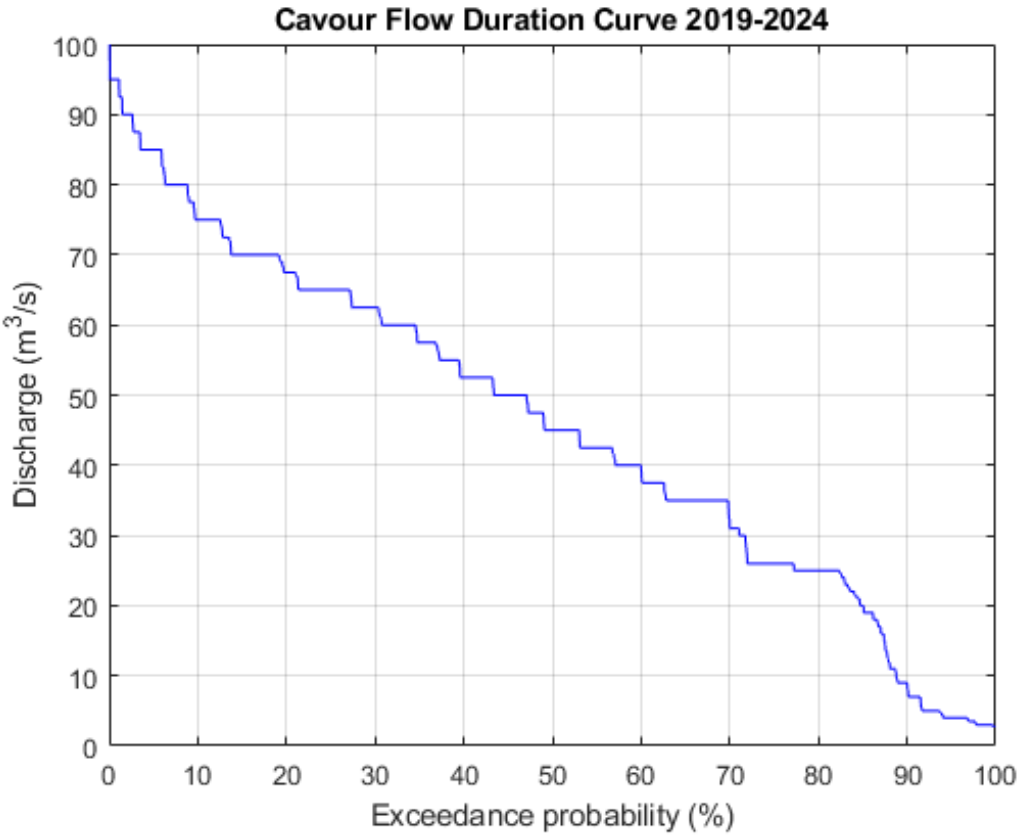

Figure 28: Cavour Flow Duration Curve

5.4 Farini and Cavour Hydrograph Comparison

It is now possible to view more in details the comparison of flow rates from the two canals. The period from 2021 to 2022 is characterized by flow shortages from the Cavour canal with an average flow rate of 37.30 m^3/s while the Farini canal has flow shortages during the years 2022 and 2023 with an average flow rate of 4.17 m^3/s. The following hydrographs highlight drought periods of the two canals. The blue line is the result of the difference of the two canals discharge and shows the amount of water provided by the Po river at the Cavour's incile in Chivasso.

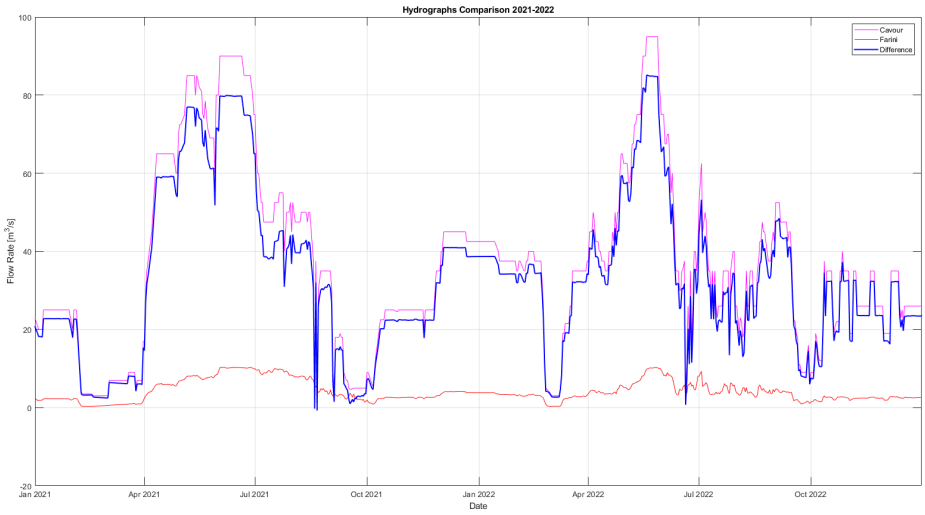

Figure 29: Farini and Cavour hydrograph comparison 2021-2022

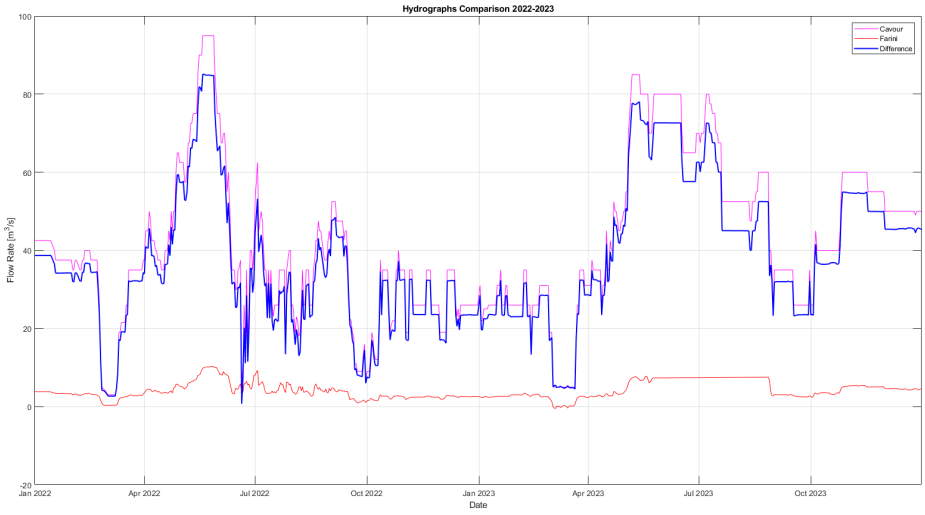

Figure 30: Farini and Cavour hydrograph comparison 2022-2023

6 The lateral outlet floodgates of the Lucca canal

6.1 Lucca canal water surface

Assuming that the Lucca canal has a rectangular floodgate, and knowing from Table 15 that its width is $b_f = 5\,m$ and from the hydrograph of Fig. 18 that its flow rate varies throughout the year but has a maximum value of 9 m^3/s, using a Manning's coefficient of $n = 0.04\,m^{1/3}/s$ for a clean canal bed with some pools and shoals and assuming also $i_f = 0.0025$, the height of the water surface level Y can be determined using the Chezy formula.

$$Q = b_f Y \frac{1}{n} \mathcal{R}^{1/6} \sqrt{\mathcal{R}\, i_f}$$

$$Q = b_f Y \frac{1}{n} \left[\frac{(b_f Y)}{(b_f + 2Y)}\right]^{1/6} \sqrt{\left[\frac{(b_f Y)}{(b_f + 2Y)}\right] i_f}$$

The results calculated are reported in the Table 7 below;

Table 7: Lucca canal water surface height

Flow rate m^3/s	Manning's n value	Width m	i_f	Water surface height m
9	0.04	5	0.0025	1.50
8	0.04	5	0.0025	1.38
7	0.04	5	0.0025	1.26
6	0.04	5	0.0025	1.13
5	0.04	5	0.0025	1.00
4	0.04	5	0.0025	0.86
3	0.04	5	0.0025	0.71
2	0.04	5	0.0025	0.55
1	0.04	5	0.0025	0.35

By introducing on HEC-RAS a model of the canal and imposing the same boundary conditions of the problem, the software calculate similar results to that obtained using Chezy's uniform flow equation reported in Tab. 7.

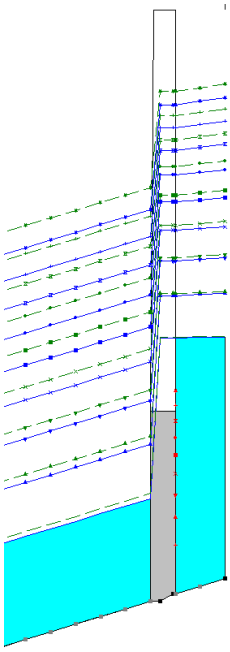

PF 1	1.00	167.38	167.71
PF 2	2.00	167.38	167.89
PF 3	3.00	167.38	168.04
PF 4	4.00	167.38	168.16
PF 5	5.00	167.38	168.28
PF 6	6.00	167.38	168.38
PF 7	7.00	167.38	168.48
PF 8	8.00	167.38	168.57
PF 9	9.00	167.38	168.66

Figure 31: W.S. Heights From HEC-RAS

Table 8: Lucca canal water surface height from HEC-RAS

Flow rate m^3/s	Water surface elevation m	Canal-bed elevation m	Water surface height m
9	168.66	167.38	1.28
8	168.57	167.38	1.19
7	168.48	167.38	1.1
6	168.38	167.38	1
5	168.28	167.38	0.9
4	168.16	167.38	0.78
3	168.04	167.38	0.66
2	167.89	167.38	0.51
1	167.71	167.38	0.33

The levels of the water surface reported on Tables 7 and 8 recur with the annual frequencies that results from the flow duration curve of the Lucca canal in Fig. 20 and are reported in the following table.

The same calculation has been repeated for the value of the Mean Annual Discharge for the Lucca canal. From Tab. 4 the observed discharge value is $5.39\,m^3/s$ and using

Table 9: Lucca Flow Duration Curve results

Flow rate Q m^3/s	Exceedance probability %	Exceedance frequency $\frac{days}{year}$
9	3.93	14
8	25.34	92
7	45.46	166
6	55.84	204
5	62.50	228
4	67.35	246
3	72.68	265
2	77.22	282
1	81.49	297

the Chezy formula, the corresponding uniform flow level is 1.05 m.

6.2 Lucca floodgate heights

The floodgate opening height adjustment of the Lucca canal allows to determine the flow rate values mentioned above; in the case of an opening height of 0.15 m the Bernoulli's theorem is applied to obtain a flow rate Q of this specific case.

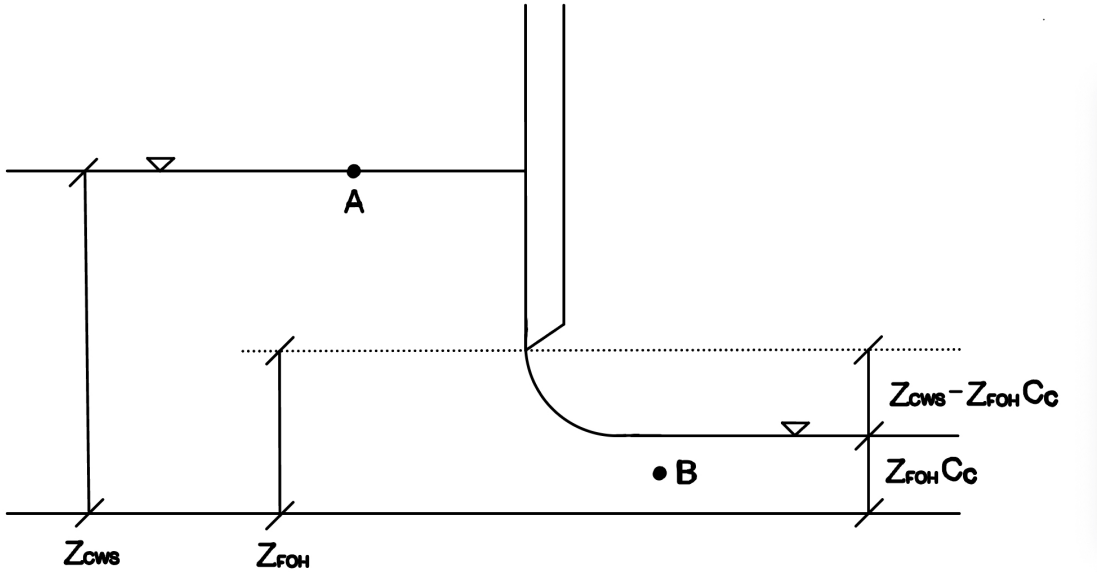

Figure 32: Floodgate Opening

$$H_A = H_B$$
$$\implies z_A + \frac{p_A}{\gamma} + \frac{U_A^2}{2g} = z_B + \frac{p_B}{\gamma} + \frac{U_B^2}{2g}$$

Two points A and B can now be chosen from the Cavour canal and the Lucca canal in order to simplify the calculations. This can be achieved by placing A on the water free-surface of the Cavour canal and B right after the contracted section created by the floodgate.

$$z_A + \frac{p_A}{\gamma} = Z_{CWS};$$
$$\frac{U_A^2}{2g} = 0$$
$$z_B + \frac{p_B}{\gamma} = C_C \, Z_{FOH}$$

Where Z_{CWS} is the water free-surface of the Cavour canal, Z_{FOH} is the opening of the floodgate and C_C the coefficient of contraction, which is assumed to be equal to 0.61. This way the Bernoulli's equation is simplified:

$$Z_{CWS} = C_C \, Z_{FOH} + \frac{U_B^2}{2g}$$

From which it is obtained the flow rate exiting the floodgate:

$$Q = U_B\,\Omega = U_B\,[C_C\,Z_{FOH}\,W]$$

Where W is the value of width taken from Tab. 7, equal to 5 m.

$$U_B = \sqrt{(Z_{CWS} - C_C\,Z_{FOH})2g}$$

$$Q = \sqrt{(Z_{CWS} - C_C\,Z_{FOH})2g}\,[C_C\,Z_{FOH}\,W]$$

Table 10: Upstream section of the Lucca canal outlet

Parameter	Value	Unit of measurement
Canal	Cavour	-
Cross section	60434	m
Flow rate	45.93	m^3/s
Water surface elevation	169.85	m
Canal bed elevation	168.50	m

By knowing from the HEC-RAS model that at the upstream section of the Lucca canal outlet, the Cavour canal has a water surface height of 169.85 m, it is obtained:

$$Z_{CWS} = 169.85 - 168.5 = 1.35\,m$$

$$Q = \sqrt{2 \cdot 9.8\,m/s^2 \cdot [1.35\,m - (0.61 \cdot 0.15\,m)]} \cdot [0.61 \cdot 0.15\,m \cdot 5\,m] = 2.27\,m^3/s$$

The previous calculation can be repeated for progressively increasing heights. The following simulation will have 5 cm increments in the floodgate opening and the results obtained are reported in Tab. 11 below.

Table 11: Floodgate height variation

Floodgate opening height m	Flow rate m^3/s
0.15	2.272
0.20	2.993
0.25	3.694
0.30	4.376
0.35	5.038
0.40	5.680
0.45	6.302
0.50	6.902
0.55	7.480

It is possible to obtain the values of height opening related to Bernoulli's equation for flow rates:

$$Q = \sqrt{(Z_{CWS} - C_C\ Z_{FOH})2g}\ [C_C\ Z_{FOH}\ W]$$

Table 12: New floodgate heights

Flow rate m^3/s	New floodgate opening height m
9.00	0.691
8.00	0.597
7.00	0.508
6.00	0.426
5.00	0.347
4.00	0.272
3.00	0.201
2.00	0.131
1.00	0.065

In order to verify the results of Tab. 12, the same calculation has been repeated with

the Bernoulli's equation for flow rates:

$$Q = \sqrt{(Z_{CWS} - C_C\, Z_{FOH})2g}\,[C_C\, Z_{FOH}\, W]$$

The new results are very similar to the old ones, proving the theoretical procedure.

Table 13: Floodgate heights verification

Floodgate opening height m	Flow rate m^3/s
0.691	8.99
0.597	8.00
0.508	7.00
0.426	6.01
0.347	5.00
0.272	4.00
0.201	3.01
0.131	1.99
0.065	1.00

At last these flow rates can be manually checked by varying the value of height opening on the HEC-RAS model iteratively. The boundary conditions are imposed equal to the ones used for the theoretical calculations, in particular, all other floodgates are closed and the Cavour canal is supplied by a flow rate of 45.93 m^3/s from the Po river.

Table 14: Floodgate heights from HEC-RAS

Floodgate opening height m	Upstream flow rate m^3/s	Downstream flow rate m^3/s	Resulting flow rate m^3/s
0.065	45.93	43.38	2.55
0.131	45.93	40.95	4.98
0.201	45.93	38.56	7.37
0.272	45.93	36.31	9.62
0.347	45.93	34.12	11.81
0.426	45.93	31.91	14.02
0.508	45.93	29.99	15.94
0.597	45.93	28.25	17.68
0.691	45.93	28.7	17.23

7 HEC-RAS Model

The HEC-RAS software allows to estimate the water discharge present at any point along the canal by performing steady-flow analyses.[17]

This is made possible through a 1D study, which involves uploading into the software a geometric model of the canal that includes the various slopes and lengths obtained from historical project plans, and introducing the corresponding cross-section for each station, derived from parameters such as bottom width, bank slope, inner embankment inclination, and crest elevation.

For data acquisition, the work carried out by the irrigation consortia proved useful, as they mapped the geographical positions of the outlet structures of the derivation canals onto a QGIS model corresponding to the two areas of the Cavour canal Authority, West and East Sesia.[18]

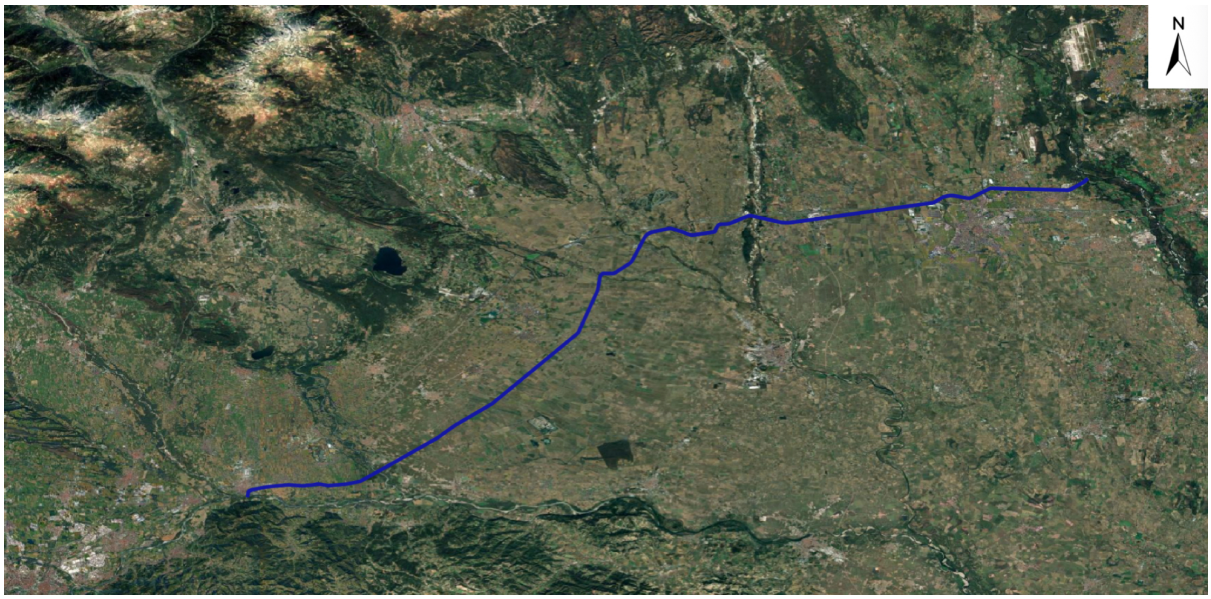

Figure 33: Cavour Canal route - 1:150000

The project originated from the analysis of the historical profiles of the canal. From these documents, the reference elevations, the elevation of the canal bed, and the characteristic slopes of the various reaches were obtained. Based on this preliminary information, it was possible to define the general geometric configuration of the hydraulic structure.

Subsequently, starting from these fundamental data, the canal cross-sections were developed in Excel. For each section, the bank slopes, the bottom widths indicated in the historical designs, and the progressive distances between the stations (moving from downstream to upstream) were used. The result was a set of geometrically consistent sections ready for integration into the model.

[17] https://www.hec.usace.army.mil/confluence/rasdocs/rasum/latest/performing-a-steady-flow-analysis

[18] https://www.estsesia.it/

Once imported into HEC-RAS, the sections were interpolated to build a one-dimensional model with regular intervals of about 240 meters, according to Samuel's equation. [19][7]

$$spacing_{max} = \frac{0.15 H_{bf}}{slope}$$

For each section, the station and elevation values of the canal crest were also defined, allowing the assignment of two Manning roughness coefficients: 0.03 for the canal bed and 0.067 for the vegetated banks. These values are taken from tables and in particular the canal bed is clean, straight, full with no rifts or deep pools and the vegetated banks usually are very weedy. [20] The Manning's n values are used by the software to model the energy losses due to friction and are necessary for the computation of the water surface elevation.

With the geometric characterization completed, multiple flow rate values taken according to the measured values of hydrograph Fig. 26, were implemented to perform a steady-flow analysis. The software then generated the longitudinal water surface profiles, providing the energy grade line for each flow scenario.

The hydraulic model was enhanced with several lateral outlet floodgates along the right bank of the Cavour canal. These include minor irrigation ditches as well as major branch canals. For the purposes of the hydraulic simulation, two key geometric parameters were reconstructed, namely the width and height of the floodgates.

The geographical position of the lateral outlets is also required to build the model; this can be estimated through the analysis of the QGIS project that contains data related to the structures and hydraulic works built for the Cavour canal. This also includes their names and locations.

QGIS therefore allows for the measurement of the distance between two points, making it possible to assign a stationing value to the various ditches. Those considered are among the most important and are listed in Table 15.

[19] https://www.hec.usace.army.mil/confluence/rasdocs/ras1dtechref/6.4/performing-a-dam-break-study-with-hec-ras/downstream-flood-routing-modeling-issues/cross-section-spacing-and-hydraulic-properties

[20] https://www.hec.usace.army.mil/confluence/rasdocs/ras1dtechref/6.6/basic-data-requirements/geometric-data/energy-loss-coefficients

Some of the implemented junctions are located on the left hydraulic bank and are defined by the intersections between the Cavour canal and the main branch canals that supply it with part of their discharge. These include the Farini canal, the Ivrea canal, the Alto Novarese subsidiary canal, and the Regina Elena canal.

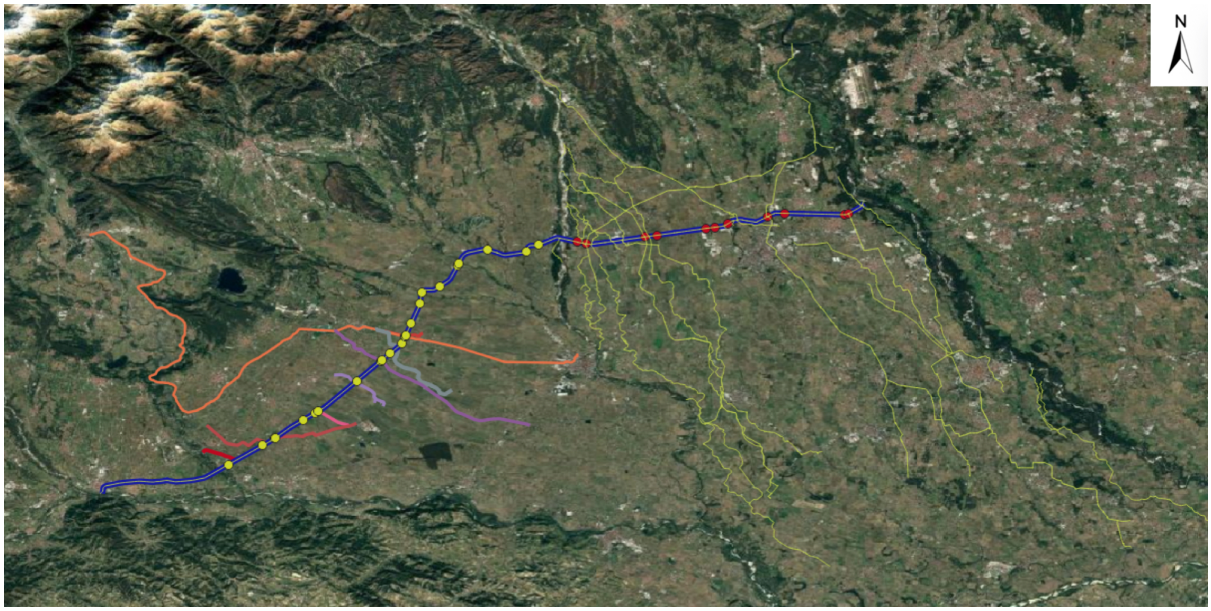

Figure 34: Canal network - 1:200000

7.1 Procedure to set up the HEC-RAS model

The first step when using HEC-RAS is that of creating the geometric model. By selecting *File → Import Geometry Data → CSV Format → Station–Elevation Format*, the geometric data were imported into the model. The creation of the Comma-Separated Values (CSV) file required particular care and proved to be the most time-consuming step, as HEC-RAS reads data according to the following order: *River Name, Reach Name, XS, Station, Elevation.*

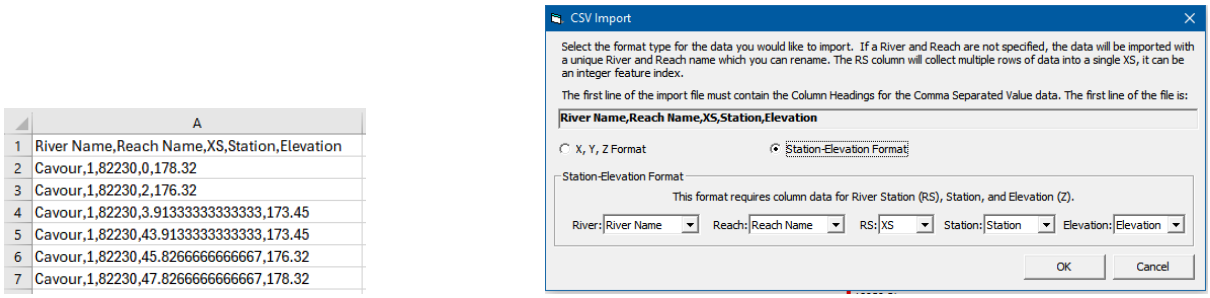

Figure 35: CSV import

Consequently, for each cross section reported in the historical design, from upstream to downstream, it was first necessary to recalculate the distances of each section starting from the downstream end and proceeding upstream to the intake structure. Using the canal slopes and widths, the cross sections were then reconstructed. Subsequently, the reach lengths table was defined, specifying for each section the distance from the immediately upstream one.

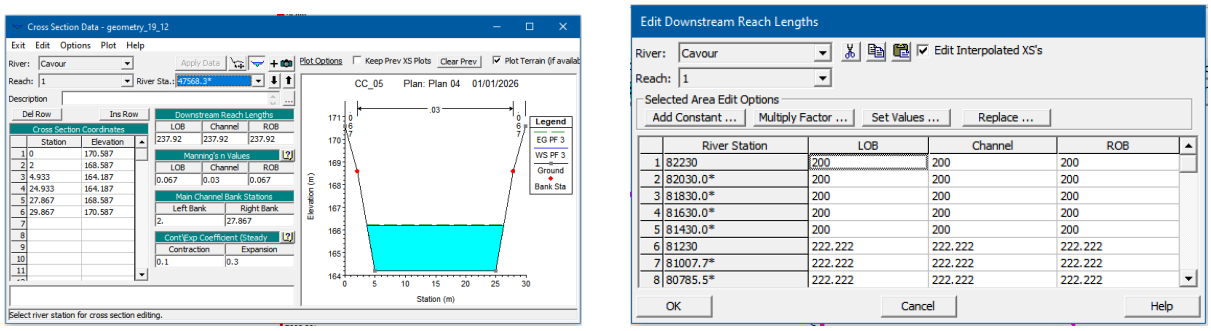

Figure 36: Reach lenghts

The bank positions were then assigned for all cross sections. The following step consisted in densifying the sections by applying Samuel's formula in order to determine the maximum allowable spacing between cross sections. [7]

Roughness values for the canal bed and banks, derived from regulatory guidelines [21], were assigned through *Tables → Edit Manning's n → Set Values.*

[21] https://www.hec.usace.army.mil/confluence/rasdocs/ras1dtechref/6.6/basic-data-requirements/geometric-data/energy-loss-coefficients

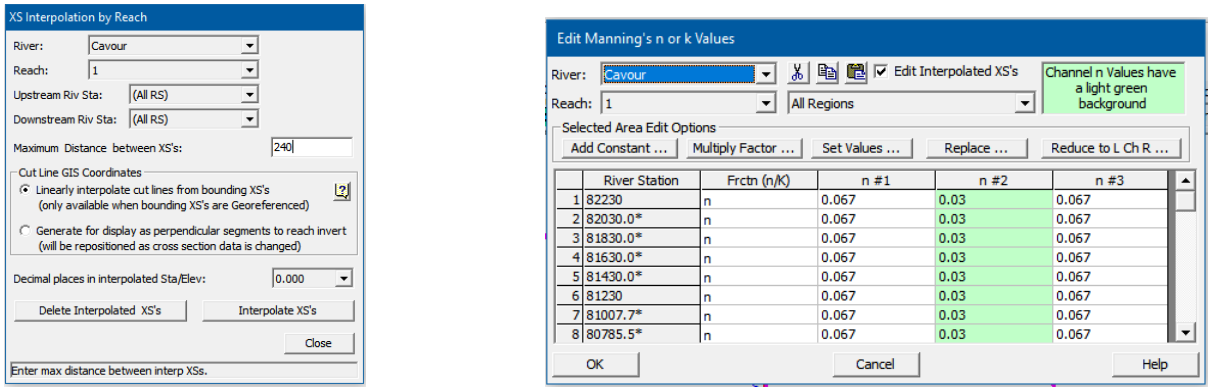

Figure 37: XS interpolation and Manning's coefficients

For the steady-flow analysis, the discharge values for the various profiles, expressed in cubic meters per second, were entered via *Edit* → *Steady Flow Data* in the main window, together with the selection of the reach boundary conditions. With regard to the inclusion of lateral outflow structures, the procedure followed was *Edit* → *Geometric Data* → *Lateral Structure* → *Options* → *Add Lateral Structure*, subsequently specifying the structure name, the corresponding station, and the geometric parameters of the weir and gates.

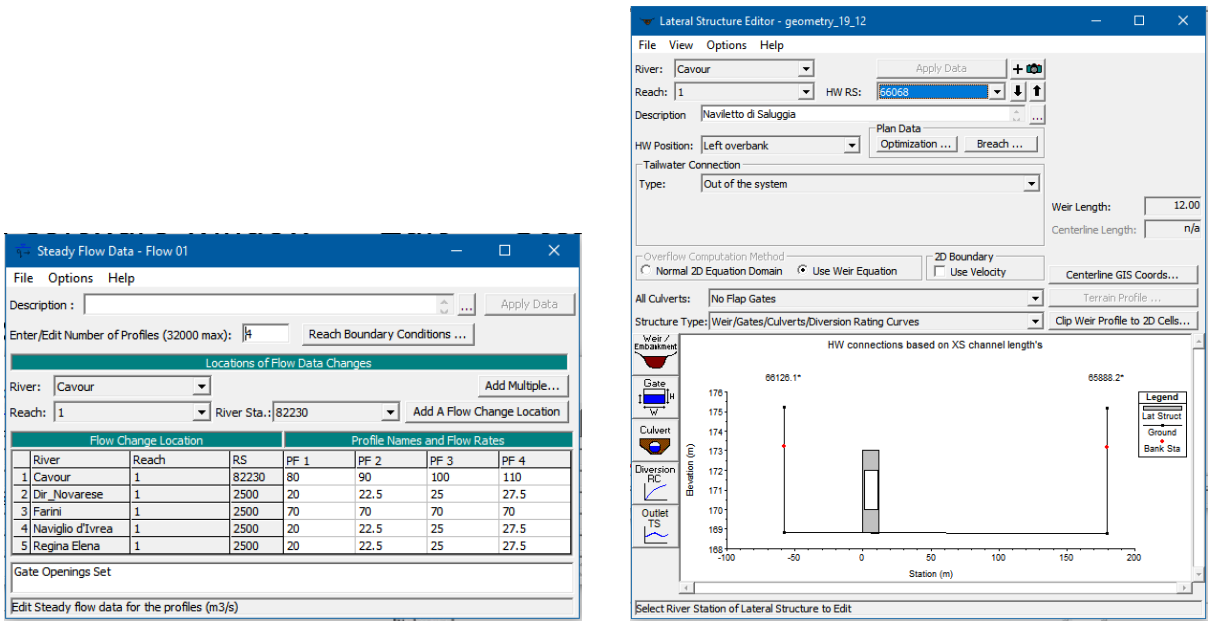

Figure 38: Steady flow data and lateral structures editor

A crucial step consisted in defining the gate openings within the Steady Flow Data window and optimizing them prior to running the steady-flow simulation Fig. 39. Provided that no errors were detected, HEC-RAS computed the hydraulic profiles, including the Energy Grade Line and the Water Surface Line, and supplied the full set of numerical results in tabular form Fig. 40, such as total discharge (Q total), minimum canal eleva-

tion, water surface elevation, energy grade elevation, energy grade slope, canal velocity, flow area, top width, and Froude number. Based on these outputs, the following plots were generated: canal velocity Fig. 42, flow area Fig. 43, and canal top width Fig. 44.

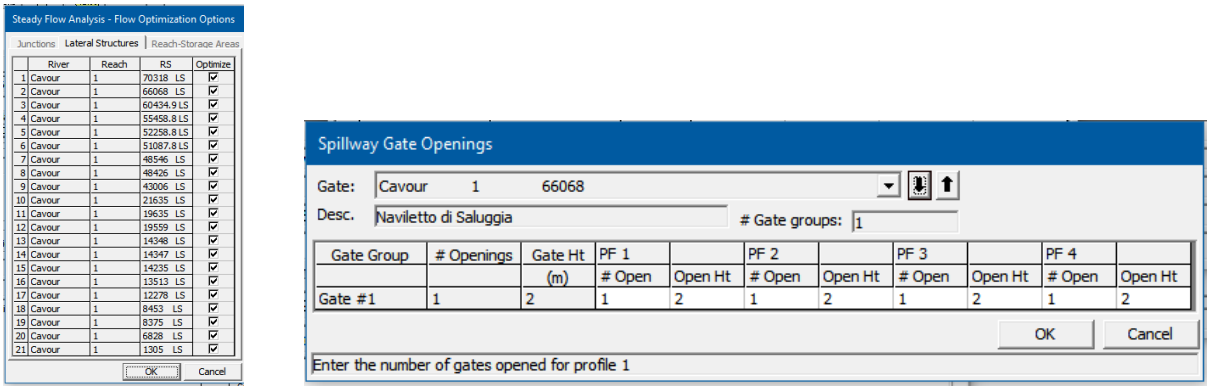

Figure 39: Outlets optimization and gate openings

The velocity graph illustrates how the water speed within the canal varies along its length. Changes in velocity reflect the influence of hydraulic conditions and canal geometry, with higher velocities typically occurring in narrower or deeper sections where the flow is more constrained. Fig. 42

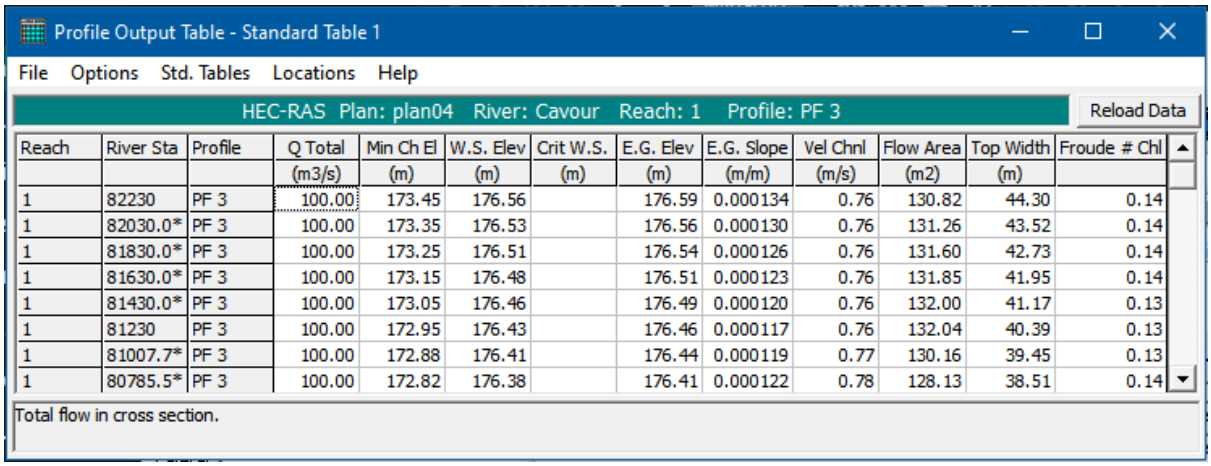

Reach	River Sta	Profile	Q Total	Min Ch El	W.S. Elev	Crit W.S.	E.G. Elev	E.G. Slope	Vel Chnl	Flow Area	Top Width	Froude # Chl
			(m3/s)	(m)	(m)	(m)	(m)	(m/m)	(m/s)	(m2)	(m)	
1	82230	PF 3	100.00	173.45	176.56		176.59	0.000134	0.76	130.82	44.30	0.14
1	82030.0*	PF 3	100.00	173.35	176.53		176.56	0.000130	0.76	131.26	43.52	0.14
1	81830.0*	PF 3	100.00	173.25	176.51		176.54	0.000126	0.76	131.60	42.73	0.14
1	81630.0*	PF 3	100.00	173.15	176.48		176.51	0.000123	0.76	131.85	41.95	0.14
1	81430.0*	PF 3	100.00	173.05	176.46		176.49	0.000120	0.76	132.00	41.17	0.13
1	81230	PF 3	100.00	172.95	176.43		176.46	0.000117	0.76	132.04	40.39	0.13
1	81007.7*	PF 3	100.00	172.88	176.41		176.44	0.000119	0.77	130.16	39.45	0.13
1	80785.5*	PF 3	100.00	172.82	176.38		176.41	0.000122	0.78	128.13	38.51	0.14

Figure 40: 1D results

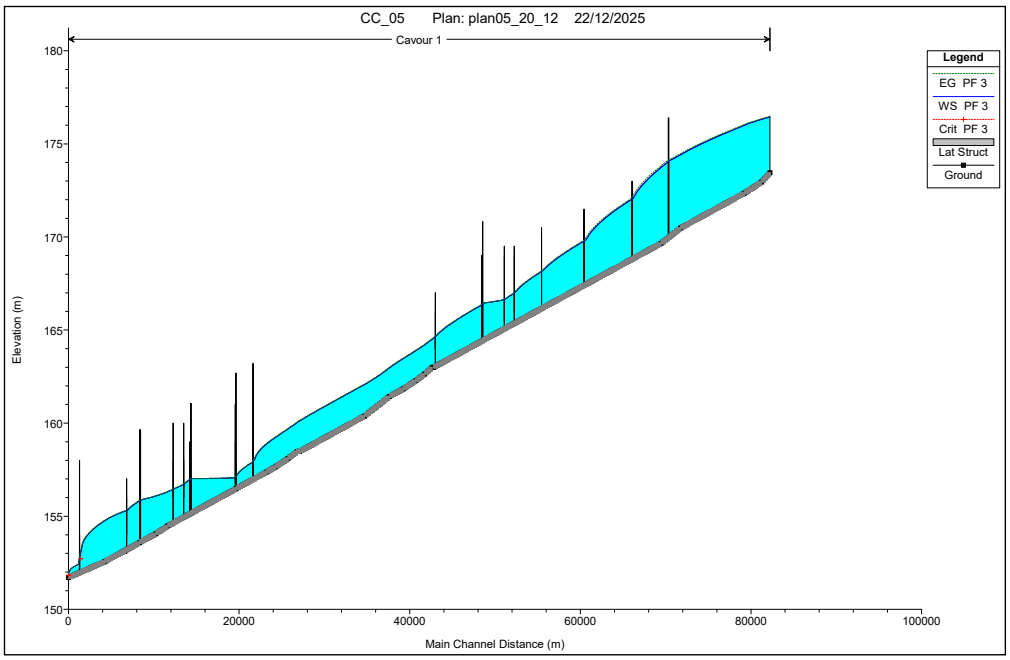

Figure 41: Canal profile example with a flow rate of 100 m^3/s

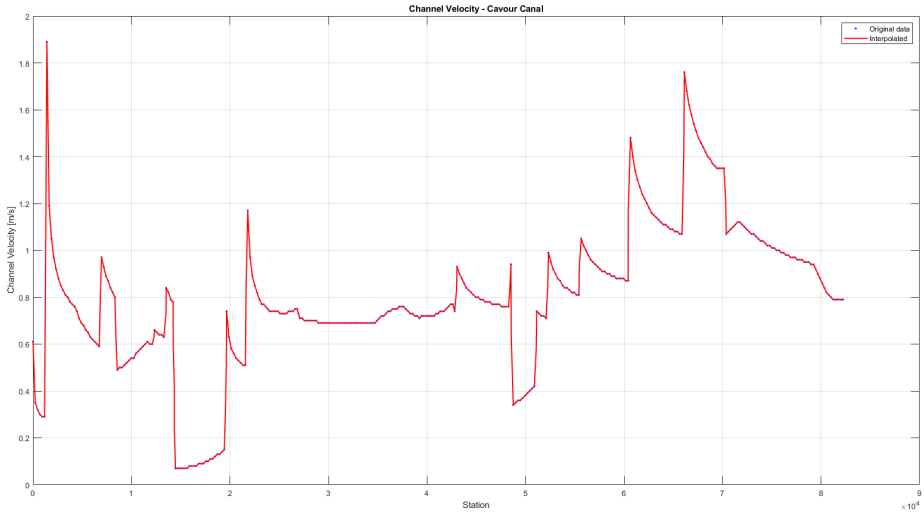

Figure 42: Canal velocity example with a flow rate of 100 m^3/s

The cross-sectional area graph shows how the flow section area of the canal changes spatially. This representation helps to understand how variations in canal shape affect the flow capacity and the distribution of water within the canal. Fig. 43

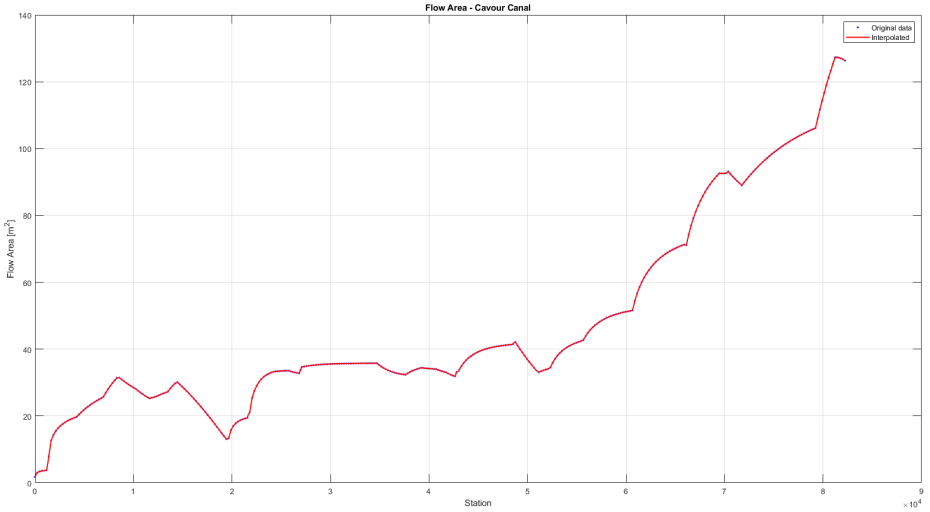

Figure 43: Canal flow area example with a flow rate of 100 m^3/s

The top-width graph describes the variation of the water surface width at the upper edge of the canal. Changes in top width are associated with differences in flow depth and side slopes, providing insight into how the canal geometry interacts with the flow regime. Fig. 44

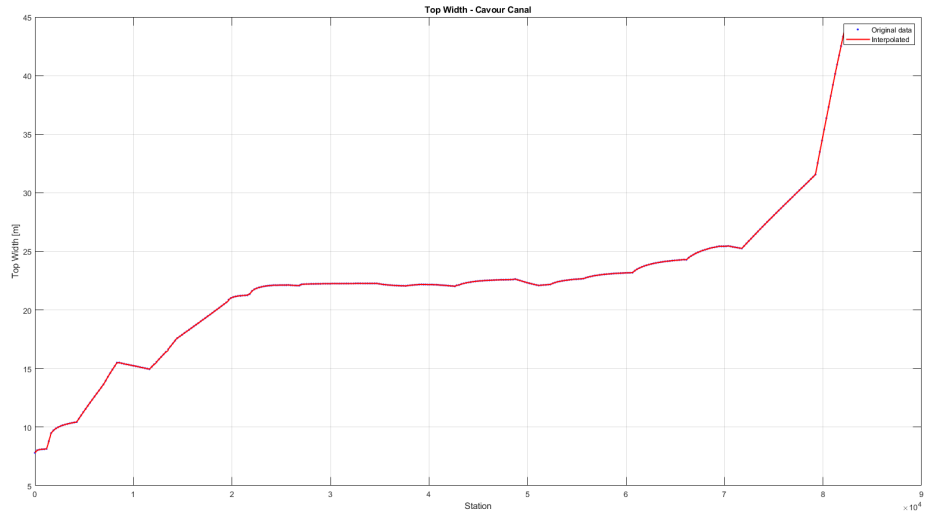

Figure 44: Canal top width example with a flow rate of 100 m^3/s

7.2 Lateral floodgate structures

For the lateral floodgate structures reported on Table 15 the following assumption are made:

Floodgates geometric parameters:

- **Width**: measured from aerial photos of the floodgates structures, marked on QGIS by the consortia and reconstructed on HEC-RAS by leaving one meter of weir embankment on each side of the lateral structure;
- **Height**: imposed equal to the height of the canal flank; the sill is set at the canal bed elevation and the floodgate develops vertically until the campaign plain elevation.

Table 15: Branch canals and subsidiaries floodgates geometric parameters

Name	Station m	Width m	Height m	Type
Farini canal	70318	35	6.4	Inlet
Lucca canal	60435	5	6.3	Outlet
Ivrea canal	48546	8.5	6.4	Inlet
Alto Novarese canal	24693	10	6.1	Inlet
Montebello canal	24693	7	6.1	Outlet
Biraga canal	21635	10	6.2	Outlet
Busca canal	19635	9	6.2	Outlet
Regina Elena canal	8453	12	6	Inlet
Quintino Sella canal	8375	8	6	Outlet
Vigevano canal	1305	14	6	Outlet

7.3 Closed floodgates case

In this case all the outlet floodgates are closed. This case verifies in the so called 'dry periods', when the branch canals are closed for maintenance works for example.[22] The flow of water of the Cavour canal is preserved from upstream to downstream not considering dissipation. These can be caused by water losses due to the poor grip of the floodgates. In the absence of precise information this assumption is neglected. With the assumption of a concession flow rate of 110 m^3/s and inflow flow rates of the subsidiary canals equal to the ones reported in Table 16 an increase in the water surface elevation is seen from the results of the model, leading to floodings.

[22] https://www.ovestsesia.it/2025/08/29/manifesto-disattivazione-degli-imbocchi-di-canali-dirrigazione/

Table 16: Flow rates from subsidiary canals

Name Canal-Ditch	Station m	Flow Rate m^3/s	Type
Cavour canal	82230	20	Inlet
Farini canal	70318	10	Inlet
Ivrea canal	48546	10	Inlet
Alto Novarese canal	24693	25	Inlet
Regina Elena canal	8453	45	Inlet

The flow rate must be calculated from downstream to upstream since downstream there are smaller canal cross sections, designed to hold less amount of water compared to the upstream one due to the distribution of water to the branch canals. For this reason if the outlet floodgates are closed and the flooding phenomenon must be avoided the flow rate needs to be verified using the Chezy equation, applied with the canal cross section geometry.

$$Q = \Omega \frac{1}{n} \mathcal{R}^{1/6} \sqrt{\mathcal{R}\, i_f}$$

Where:

$$\alpha = arctan \frac{2}{3}$$

$$\Omega = Y\, b_f + Y^2\, tan\, \alpha$$

$$\mathcal{P} = 2\frac{Y tan\, \alpha}{sin\, \alpha} + b$$

$$\mathcal{R} = \frac{\Omega}{\mathcal{P}} = \frac{Y\, b_f + Y^2\, tan\, \alpha}{2\frac{Y tan\, \alpha}{sin\, \alpha} + b}$$

$$Q = [Yb + Y^2 tan\, \alpha] \frac{1}{n} \left[\frac{Yb + Y^2 tan\, \alpha}{2\frac{Y tan\, \alpha}{sin\, \alpha} + b} \right]^{\frac{1}{6}} \sqrt{\left[\frac{Yb + Y^2 tan\, \alpha}{2\frac{Y tan\, \alpha}{sin\, \alpha} + b} \right] i_f}$$

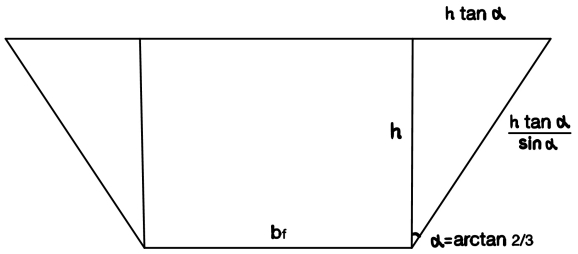

Figure 45: Cross section example

Table 17: Downstream flow rates

Parameter	Value	Unit of measurement
Maximum main canal depth Y	4	m
canal bed width b_f	7.5	m
Bank inclination α	33.69	$degrees$
Manning roughness coefficient n	0.03	$m^{1/3}/s$
canal bed slope i_f	0.00025	m/m

Assuming:

The resulting flow rate is 38.16 m^3/s which is less than the concession flow rate. The opening of branch canals is required to avoid floodings.

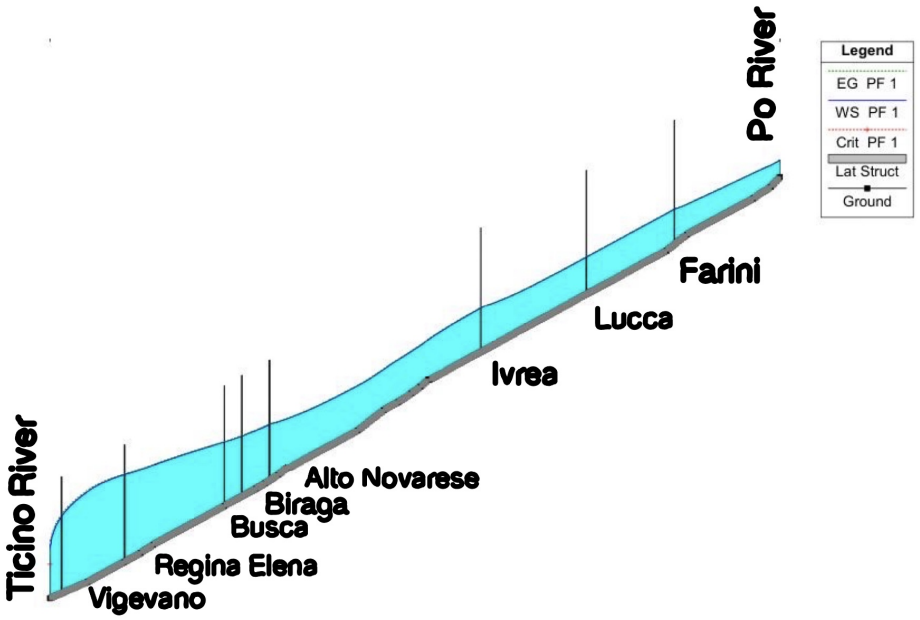

Figure 46: Closed floodgates case

7.4 Open floodgates case

7.4.1 Closed subsidiary canals case

In the open floodgate case scenario all the canal's outflow floodgates are opened with maximum opening height, which is equal to that reported on Table 15. This case study involves the closure of all subsidiary canals and this time, the case study analyzes a maximum flow rate taken from the Po River that reaches the concession value of 110 m^3/s. In this case, it can be observed how the distribution of water favors the upstream branch canals, which belong to the Ovest Sesia consortium, and the water level of the Cavour canal drops along its route, resulting in a lack of water in the final stretch.

Table 18: Derivation flow rates with closed subsidiary canals

Name Canal-Ditch	Station m	Flow Rate m^3/s	Type
Lucca canal	60435	69.87	Outlet
Montebello canal	24693	18.80	Outlet
Biraga canal	21635	12.83	Outlet
Busca canal	19635	5.76	Outlet
Quintino Sella canal	8375	2.63	Outlet
Vigevano canal	1305	0	Outlet

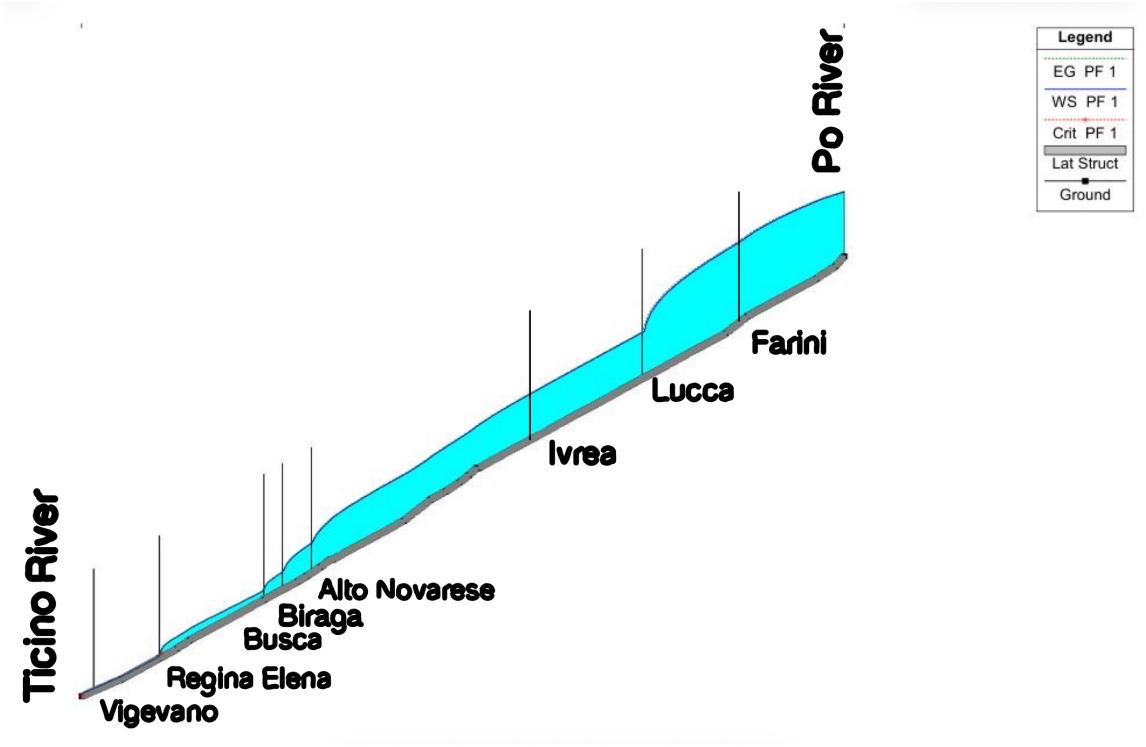

Figure 47: Open floodgates case

7.4.2 Realistic opening scenario

This scenario simulates the opening of both the outflow outlets for the distribution of water to the branch canals, and the activation of the main hydraulic nodes, for the supply of water to the Cavour canal.

Lets start by simulating inflow rates equal to those reported in Tab. 16 to reach the concession flow rate of 110 m^3/s.

As a further assumption, also in this case all the outlets are open with maximum opening height, reported in Table 17. The derivation flow rate in this case is also given by the equation:

$$Q_{derivation} = Q_{upstream} - Q_{downstream}$$

By opening the outlet floodgates and the inlet hydraulic nodes, the two extreme cases of flooding and lack of water in the downstream sections of the Cavour canal are avoided.

Table 19: Realistic derivation flow rates

Name Canal-Ditch	Station m	Flow Rate m^3/s	Type
Lucca canal	60435	19.29	Outlet
Montebello canal	24693	20.68	Outlet
Biraga canal	21635	14.95	Outlet
Busca canal	19635	8.02	Outlet
Quintino Sella canal	8375	8.09	Outlet
Vigevano canal	1305	32.58	Outlet

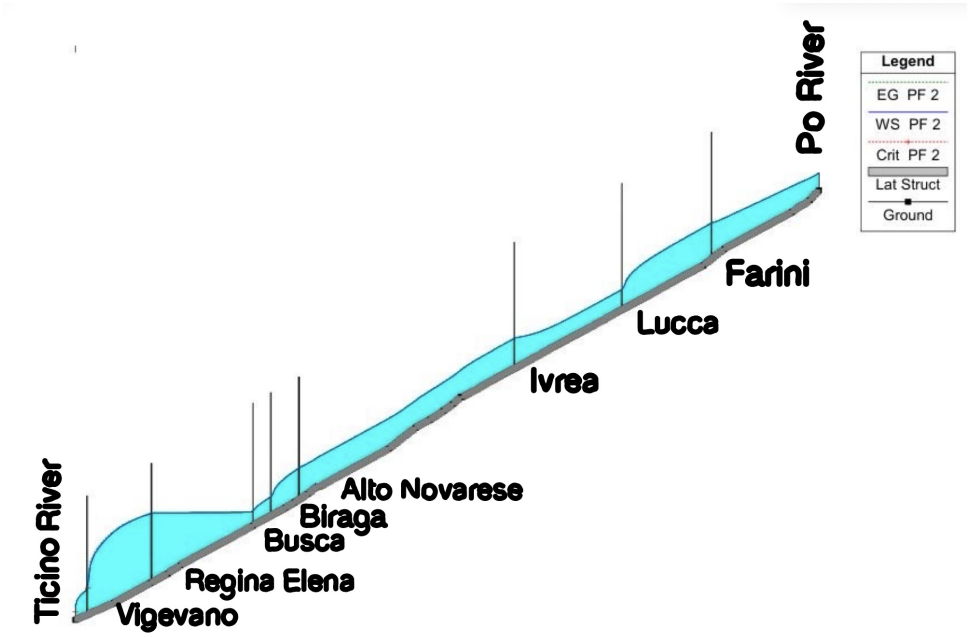

Figure 48: Realistic opening scenario

8 Summary

From the hydrograph of the Cavour Canal Fig.26, it can be observed that the discharge of the Cavour Canal varies seasonally, ranging from a minimum of about 2.8 m^3/s to a maximum of about 100 m^3/s.

The two-year period with the lowest discharges was 2021–2022, with an average flow of approximately 37 m^3/s. Considering all the available data, the overall annual average discharge is about 46 m^3/s. Tab. 6

From the regime curves, it emerges that the highest discharges occur during the summer months. In particular, May consistently shows values above 65 m^3/s, while winter months are characterized by lower flows, generally below 30 m^3/s. Figures 19, 23 and 27.

The Farini canal contribution averages 4.95 m^3/s, with seasonal maximum values in June and minimum values in February, ranging from 0 to about 11 m^3/s. Tab. 5

After subtracting the water coming from the Dora Baltea river of the Farini canal, from the Cavour Canal discharge, it appears that the Po River provided a discharge greater than 80 m^3/s only once, during the 2022 drought period. Figures 29 and 30

The Lucca Canal shows discharges ranging from 1 to 9 m^3/s, with an annual average of about 5.4 m^3/s Tab.4

Since the Lucca canal is supplied by the Cavour canal, its discharge was calculated from the Cavour canal water levels using the Bernoulli theorem. Considering the Cavour canal with an average discharge of 45.93 m^3/s, two types of results were obtained depending on the floodgate opening. For example, with a 0.40 m gate opening, the calculated discharge is 5.68 m^3/s, which approximates the annual average and from the frequency curve it can be seen that this flow rate value is exceeded for 230 days every year Fig. 20

The HEC-RAS simulations allowed for the comparison of real data and the analysis of various case studies, such as the opening and closing of the floodgates discussed previously. Specifically, the Table 19 shows the results of the simulations of the flow rates of the realistic case, which approximate those hypothesized in Chapter 4.